THESIS – TM 185400

# NUMERICAL AND EXPERIMENT INVESTIGATION OF THE HEAT-TREATED SPUR GEAR FOR APPLICATION IN THE INDUSTRIAL MECHANICAL PRESS

IMANG EKO SAPUTRO
02111850080006

*Supervisor*
Alief Wikarta, ST., MSc.Eng., Ph.D.

Mechanical Engineering Department
Faculty of Industrial and Systems Engineering
Institut Teknologi Sepuluh Nopember
2020

THESIS – TM 185400

# NUMERICAL AND EXPERIMENT INVESTIGATION OF THE HEAT-TREATED SPUR GEAR FOR APPLICATION IN THE INDUSTRIAL MECHANICAL PRESS

IMANG EKO SAPUTRO
02111850080006

*Supervisor*
Alief Wikarta, ST., MSc.Eng., Ph.D.

Mechanical Engineering Department
Faculty of Industrial and Systems Engineering
Institut Teknologi Sepuluh Nopember 2020

TESIS – TM 185400

# INVESTIGASI NUMERIK DAN EKSPERIMEN PADA *SPUR GEAR* DENGAN PERLAKUAN PANAS UNTUK PENGGUNAAN DALAM MESIN *PRESS* MEKANIK

IMANG EKO SAPUTRO
02111850080006

*Dosen Pembimbing*
Alief Wikarta, ST., MSc.Eng., Ph.D.

Departemen Teknik Mesin
Fakultas Teknologi Industri dan Rekayasa Sistem
Institut Teknologi Sepuluh Nopember
2020

**THESIS APPROVAL SHEET**

This thesis is written to fulfill one of the prerequisites in obtaining the following degree

**Magister Teknik (M.T.)**

at

**Institut Teknologi Sepuluh Nopember**

by:

**Imang Eko Saputro**
**NRP: 02111850080006**

Date of Examination: July 22nd, 2020
Graduation Period: September 2020

Approved by:

**Supervisors:**

1. Alief Wikarta, ST., MSc.Eng., Ph.D.
   NIP. 198202102006041002 ...............................................

**Examiners:**

1. Dr. Ir. Agus Sigit Pramono, DEA.
   NIP. 196508101991021001 ...............................................
2. Achmad Syaifudin, S.T., M.Eng., Ph.D.
   NIP. 197909262005011001 ...............................................
3. Dr. Eng. Yohanes, S.T., M.Sc.
   NIP. 198006272012121003 ...............................................

Head of Mechanical Engineering Department
Faculty of Industrial Technology and System Engineering

KEMENTERIAN PENDIDIKAN DAN KEBUDAYAAN
INSTITUT TEKNOLOGI SEPULUH NOPEMBER
FAKULTAS TEKNOLOGI INDUSTRI DAN REKAYASA SISTEM
DEPARTEMEN TEKNIK MESIN

Dr.Ir.Atok Setiyawan, M.Eng.Sc.
NIP. 196604021989031002

**LEMBAR PENGESAHAN TESIS**

Tesis disusun untuk memenuhi salah satu syarat memperoleh gear

**Magister Teknik (M.T.)**

di

**Institut Teknologi Sepuluh Nopember**

oleh:

**Imang Eko Saputro**
**NRP: 02111850080006**

Tanggal Ujian: 22 Juli 2020
Periode Wisuda: September 2020

Disetujui Oleh:

**Pembimbing:**

1. Alief Wikarta, ST., MSc.Eng., Ph.D.
   NIP. 198202102006041002 ...............................................

**Penguji:**

1. Dr. Ir. Agus Sigit Pramono, DEA.
   NIP. 196508101991021001 ...............................................
2. Achmad Syaifudin, S.T., M.Eng., Ph.D.
   NIP. 197909262005011001 ...............................................
3. Dr. Eng. Yohanes, S.T., M.Sc.
   NIP. 198006272012121003 ...............................................

Kepala Departemen Teknik Mesin
Fakultas Teknologi Industri dan Rekayasa Sistem

Dr.Ir. Atok Setiyawan, M.Eng.Sc.
NIP. 196604021989031002

**Numerical and Experiment Investigation of The Heat-treated Spur Gear for Application in the Industrial Mechanical Press**

Name : Imang Eko Saputro
NRP : 02111850080006
Supervisor : Alief Wikarta, ST., MSc.Eng., Ph.D.

## ABSTRACT

Gear system is one of most common mechanical parts for machinery, such as mechanical press machine. Wear resistance and fatigue resistance of the teeth are the most critical factors influencing gear life and can be improved using heat treatment process. To improve wear resistance, the achievement of desired hardenability is the main goal. Therefore, the steel hardening technique such as induction hardening (commonly used in gear) and quenching process takes an important role for this treatment. However, traditional physical testing for optimizing heat treatment techniques must be obtained at the expense of large amounts of labor and materials. Numerical simulation, an economic alternative technique which is based on some physical models and by combining with some numerical calculation methods can become breakthrough solution for those numerous heat treatment tests.

A numerical method is built to simulate the induction hardening-heat treatment process of the spur gear. The evolution of temperature, phase transformation, and residual stress distribution of gear tooth have been studied according to the simulation results. The hardness experimental validation is also conducted to analyze the accuracy of the numerical method.

As the results, the numerical method is not too accurate in predicting the real hardness distribution due to some issues such as measurement error, parameter data mismatch between simulation and real case, and skin depth phenomenon in induction hardening which is difficult to be implemented in numerical method.

Cooling time during quenching takes a big role on the distribution of martensite evolution and the hardening depth, the higher heat transfer coefficient of quenchant does not increase the maximum hardness value, but shorten the quenching time to reach it, quenching process left massive compressive residual stresses in the root of gear teeth and tensile residual stresses in the tip of gear teeth, design of gear influence the distortion in the gear geometry.

**Keywords:** hardenability, heat treatment, induction hardening, mechanical press machine, numerical simulation, quenching, residual stress, skin depth, steel hardening

**Investigasi Numerik dan Eksperimen pada *Spur Gear* dengan Perlakuan Panas untuk Penggunaan dalam Mesin *Press* Mekanik**

Nama : Imang Eko Saputro
NRP : 02111850080006
Pembimbing : Alief Wikarta, ST., MSc.Eng., Ph.D.

## ABSTRAK

Sistem roda gigi adalah komponen mekanik yang paling sering digunakan pada permesinan, antara lain mesin *press* mekanik. Ketahanan terhadap aus dan beban letih (*fatigue*) pada gigi adalah faktor yang paling penting dalam mempengaruhi umur roda gigi yang mana bisa ditingkatkan dengan proses perlakuan panas. Pencapaian pada *hardenability* yang diinginkan adalah tujuan utama dalam proses ini. Oleh karena itu teknik pengerasan logam (*steel hardening*) seperti *induction hardening* (umum diterapkan pada roda gigi) dan proses *quenching* memegang peranan penting pada proses tersebut. Akan tetapi, uji fisik secara traditional dalam mengoptimasi teknik-teknik perlakuan panas ini harus didapatkan dengan jumlah material dan pekerja yang sangat besar. Simulasi numerik, sebuah metode alternatif yang lebih ekonomis dimana didasarkan pada beberapa permodelan fisis dan dikombinasikan dengan beberapa metode kalkulasi numerik bisa menjadi solusi terobosan akan banyaknya uji perlakuan panas yang harus dilakukan tersebut.

Sebuah metode numerik dibangun untuk mensimulasikan proses perlakuan panas-dengan induksi terhadap roda gigi jenis *spur gear*. Evolusi temperatur, transformasi fase, dan distribusi tegangan sisa pada gigi diteliti berdasarkan pada hasil-hasil simulasi. Validasi kekerasan (*hardness*) secara uji eksperimen juga dilakukan untuk menganalisa akurasi daripada metode numerik tersebut.

Dan hasilnya, metode numerik tersebut kurang akurat dalam memprediksi hasil eksperimen distribusi kekerasan disebabkan oleh beberapa isu, antara lain kesalahan pengukuran, tidak sebandingnya data parameter antara simulasi dan kondisi lapangan, dan adanya fenomena *skin depth* pada proses *induction* *hardening* yang mana sangat sulit untuk diimplementasikan pada metode numerik tersebut. Waktu pendinginan selama quenching memegang peranan besar pada hasil distribusi martensite dan kedalaman pengerasan (*hardening depth*), *quenchant* dengan koefisien penghantar panas lebih besar tidak meningkatkan nilai maksimum kekerasan tetapi memperpendek waktu quenching dalam mencapai nilai maksimum tersebut, proses *quenching* menghasilkan tegangan-tegangan sisa kompresif yang sangat besar pada daerah lembah gigi dan tegangan sisa jenis tarik pada daerah puncak gigi, desain geometris dari roda gigi dapat mempengaruhi kerusakan saat proses perlakuan panas.

**Kata Kunci:** *hardenability*, perlakuan panas, *induction hardening*, mesin *press* mekanik, simulasi numerik, *quenching*, tegangan sisa, *skin depth*, pengerasan logam

# FOREWARD

The author would like to thank the SEYI (Shieh Yih) Machinery Industry Co., Ltd, Taiwan for providing some parameter data in their industrial mechanical press and conducting experiment validation.

The author would also like to share the deepest gratitude to Alief Wikarta, ST., MSc.Eng., Ph.D. and Prof. Yiin-kuen, Fuh from National Central University, Taiwan for their supervision in this research.

*(This page is left intentionally blank)*

# Contents

# List of Figures

*(This page is left intentionally blank)*

# List of Tables

# CHAPTER 1
# INTRODUCTION

## 1.1 Background

Gear system is one of most common mechanical parts for machinery and mechanical equipment which transmits torque and power by means of the teeth engagement. Wear resistance and fatigue resistance of the gear teeth are the most critical factors influencing gear life, especially for the heavy-loaded gear such as gears in the mechanical press machine shown in the figure 1.1. Those factors can be improved using heat treatment process on the gear teeth. To improve the wear resistance, the achievement of desired hardness distributions of the teeth or well known as hardenability is the main goal of this process. There are several hardening techniques used on the gear teeth nowadays, and the most common one is induction hardening which consist of two stages such as induction heating and rapid cooling (quenching). However, the steel hardening process such as quenching is a complex and uneasy-controlled process which is associated with the major cause of residual stress-induced cracking (Şimşir & Gűr, 2008) and dimensional changes which is subjected to a further costly and time-consuming process such as straightening or hard machining to correct the part distortion and meet the final tolerance requirements (Haimbaugh, 2001). Every parameter of heat treatment needs to be studied by numerous testing to establish better quality products. However, traditional physical testing to study the effect of each parameter on final heat treatment product must be obtained at the expense of large amounts of labor and materials. Numerical simulation, an economic alternative technique which is based on some physical models and by combining with some numerical calculation methods can become breakthrough solution for those numerous heat treatment tests (Song, et al., 2007). A number of studies have been conducted to simulate quenching process on gear using finite element software, such as Song et al used ANSYS software to simulate

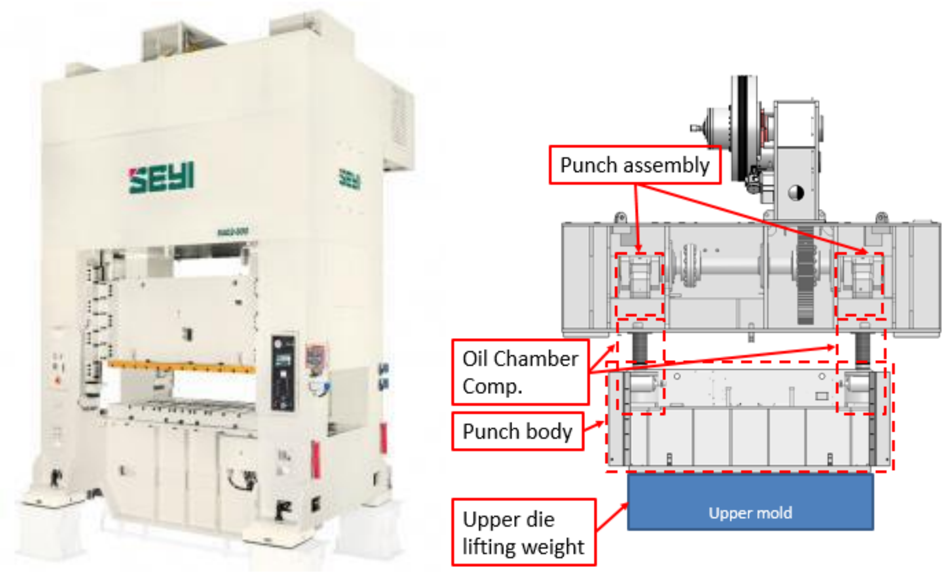


Figure 1.1 Straight side crank mechanical press machine

and analyze the surface quenching of a spur gear, and obtained the results of temperature field, thermal stress and thermal deformation in the quenching process of the spur gear (Song, et al., 2015). Zhang et al conducted simulation analysis on the quenching process of a cylindrical gear. The conclusions are that the tooth center temperature of the cylindrical gear is the highest, the tooth top temperature is the lowest, and the stress is mainly concentrated in the tooth root (Zhang, et al., 2016). Wang et al summarized the shortcomings of traditional quenching process; combined with the computer simulation technology, put forward the numerical simulation of gear carburizing and quenching process as the development direction of the current industry (Wang, et al., 2019).

### 1.2 Problem Statement

Problem statement for this research are as follows:

1. How is the accuracy of the numerical method in predicting the real heat treatment results?
2. How are the effects of quenching time and quenching medium (quenchant) to the hardness evolution of gear teeth.
3. How are the effects of quenching process to the residual stresses distribution of gear.

4. How are the effects of mass-reduction hole geometry of gear to the distortion or volume changes.

## 1.3 Scope of Problem

The scope of the problems in numerical method is limited to, along with assumptions as follows:

1. The heating and cooling process are only subjected to the surface contour of gear teeth
2. The heat transfer between heated tooth and unheated tooth next to it is neglected
3. Heat induced by deformation phenomenon is neglected
4. Some of physical and mechanical properties are not obtained from material test, but from reference paper or calculation software

## 1.4 Problem Statement

The objectives of this research project are as follows:

1. Measure the accuracy of the numerical method in predicting the real heat treatment results.
2. Investigate the effect of quenching time and quenching medium (quenchant) to the hardness evolution of gear teeth.
3. Investigate the effect of quenching process to the residual stresses distribution of gear.
4. Investigate the effect of mass-reduction hole geometry of gear to the distortion or volume changes.

## 1.5 Significance and Contribution of the Research

The significance of the research is both in the numerical and experiment method. This research established the induction hardening in the large-sized spur gear where induction hardening should be done tooth by tooth using induction block. More specifically, this research focus on gear which is commonly used in the mechanical press machine. Therefore, induction design, procedure, and numerical method are suitable for spur gears in the application of mechanical press machine.

# CHAPTER 2
# LITERATURE REVIEW AND THEORETICAL BACKGROUND

## 2.1 Literature Review

### 3.1.1 Austenitizing Process

Heat treatment process are always initiated by austenitizing process. Austenitizing is process of heating steel to certain temperature above austenite temperature then holding it for several minutes (soaking) in order to ensure uniformity of austenite phase entire volume. Because as we know that austenite phase is an unstable phase that can be transformed to other phase, such as ferrite, pearlite, bainite, and martensite by cooling process. The austenite temperature of steel depends on its carbon composition as shown iron-carbon diagram in the figure 2.1, and beside that the alloying element addition of steel also influence the minimum austenite temperature (eutectoid temperature) as shown in the figure 2.2.

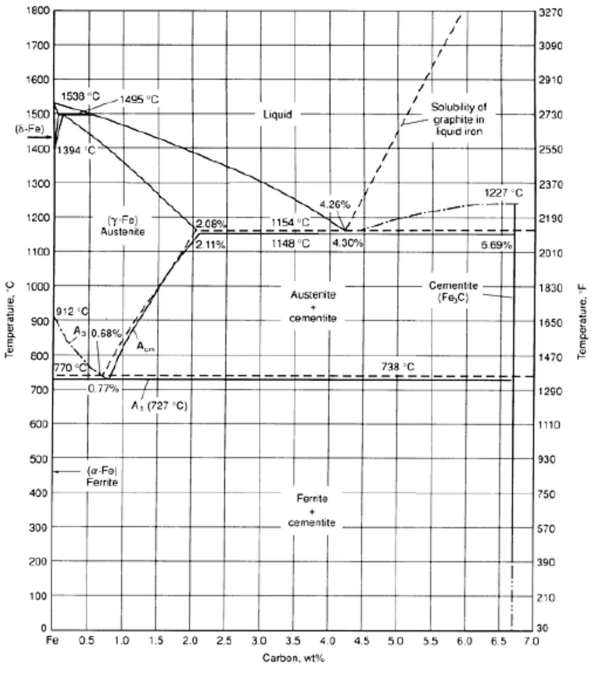


Figure 2.1. Iron-carbon equilibrium diagram up to 6.67 w% C (American Society for Metals, 1973)

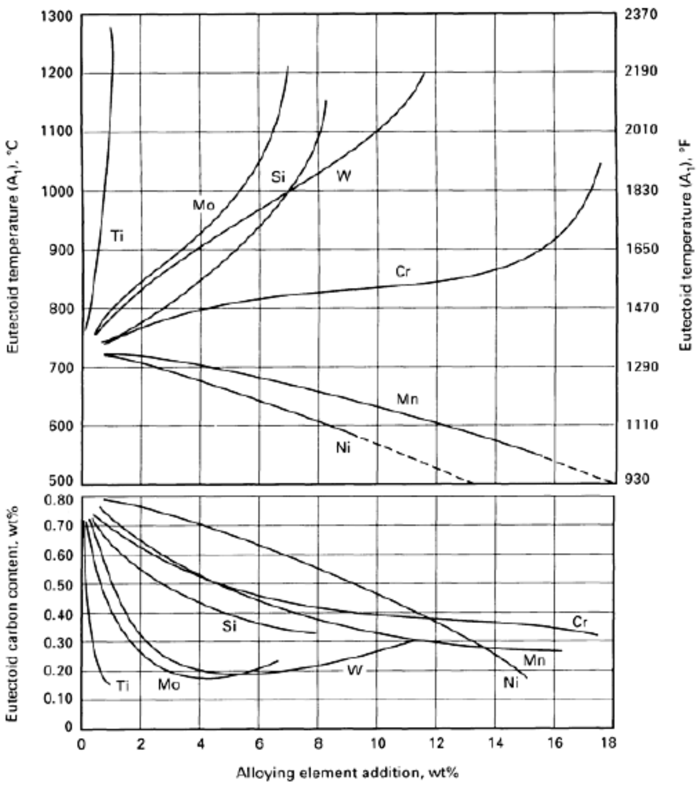


Figure 2.2. Influence of alloying element additions on eutectoid temperature and eutectoid carbon content (Bain & Paxton, 1961)

Some researches show that the rate of heating is not particularly important unless a gear is in a highly stressed condition due to previous works. If the gear is in the highly stressed, the heating rate should be slow and preheating before austenitizing is needed to minimize distortion or even cracking during austenitizing process. Preheating is done at temperature below eutectoid temperature (commonly at $720^0$C or $1330^0$F) and soaking for several minutes to ensure entire highly stressed regions getting softer (Rakhit, 2000).

### 3.1.2 Quenching Process

Quenching refers to the process of rapidly cooling metal parts from the austenitizing or solution treating temperature, typically from within the range of 815 to $870^0$C (1500 to $1600^0$F) for steel in order to generate phase transformation from austenite phase to other phases, such as ferrite, pearlite, bainite, and martensite. Stainless and high-alloy steels may be quenched to minimize the presence of grain boundary carbides or to improve the ferrite distribution but most steels including carbon, low-alloy, and tool steels, are quenched to produce controlled amounts of martensite in the microstructure (American Society for Metals, 1991).

Heat transfer during quenching occurs via all possible heat transfer mechanisms, i.e., conduction, convection and radiation. Basically, heat is removed from the surface of the specimen by convective heat transfer to the quenchant and by radiation, which results in thermal gradients driving the conduction inside the component. Convective heat transfer to the quenchant is the most important heat transfer mechanism during immersion quenching. As the component is immersed into the quenchant, the initial temperature of the component is generally well above the boiling point of the quenchant.

When a steel component is quenched, at the initial stage of quenching, austenite cools down without phase transformations. The surface of the component cools down faster than the core due to large thermal gradients. Hence, surface contracts faster than the core, leading to generation of tensile type of stresses on the surface. On the other hand, the core loads in compression to balance the stress state on the surface. Thermal stresses build in this stage may even cause non-uniform plastic flow in soft austenite. Second stage of quenching starts as soon as the martensitic transformation starts on the surface. Dilatational phase transformation strains and transformation plasticity causes a fast unloading and reverse loading on the surface. Untransformed regions react to balance those stresses. Large compressive stresses are built on the surface in this stage. The third stage in the quenching starts as soon as the phase transformations start at the core. During this stage, already transformed regions experience thermal contraction as they cool down, whereas, the transforming regions expands due to transformations. Similar to previous stage, this causes an unloading and reverse loading. Already transformed regions are loaded in tension while the transforming regions are loaded in compression (Şimşir & Gűr, 2008).

### 3.1.3 Residual Stress Due to Heat Treating

Residual stresses are stresses that exist in a solid body without an imposed external force. Factors such as cold working, phase changes while heat treating, and temperature gradients that occur during heating or cooling produce the stresses. The nature of stresses in a workpiece can influence distortion and cracking tendencies during heating and quenching. Heat treatment can result in the development of residual stresses (both compressive and tensile), dimensional change (with respect to size and shape), and quench cracking. The major benefit of reduction of the overall residual stresses in a part is the elimination of dimensional change during manufacturing. The major benefit of producing compressive residual stress through heat treatment includes improved fatigue life and increased resistance to crack initiation. Tensile residual stresses at the surface of a part are generally undesirable because they can effectively increase the stress levels, as well as cause fatigue failure, quench cracks, grinding checks, and reduce the strength of a part. Excessive tensile residual stresses in the interior of a component may also be damaging because of the existence and consequence of defects that serve as stress raisers. Subsurface quench cracks can initiate due to excessive tensile stresses.

Figure 2.3 shows the stresses at the surface of a carbon steel cylinder during heating and quenching. During heating, the surface remains in compression until the temperature reaches 1000 °C (1830 °F) when the surface becomes plastic. During cooling, the surface stresses are in tension until the surface is in the martensite formation range. The level of stress produced depends on the modulus of elasticity and the thermal coefficient of expansion of the material. The resultant net residual stresses in the part after cooling depend on the contraction of the core and its effect on contraction of the surface. If the parts are case hardened fast enough so that the core has little heat, the core may have little effect on surface stresses. If the part is through heated so that the core has heat and can contract when cooled, there may be substantial effect.

The final residual stress distribution is more complex when the quenched parts undergo phase transformation to martensite. During martensite transformation, there is an approximate increase in volume of 4% times the carbon content. The area that is martensitic tries to increase in size, producing the compressive stress as the core cools. Surfaces can quench in tension when there is very little temperature variation between the surface and center of the part. The change in stresses due to thermal volume are independent of the changes caused by phase formation, that is the major reason why the residual stress distribution is getting more complex. Figure 2.4 illustrates the complex pattern of residual stress distribution over the diameter of a quenched bar, showing residual stresses after quenching in the longitudinal and radial directions in relationship to the coil and area heated. In some particular conditions, the volumetric changes can produce sufficiently large residual stresses that can cause plastic deformation on cooling, leading to warping or distortion of the steel part (American Society for Metals, 1997).

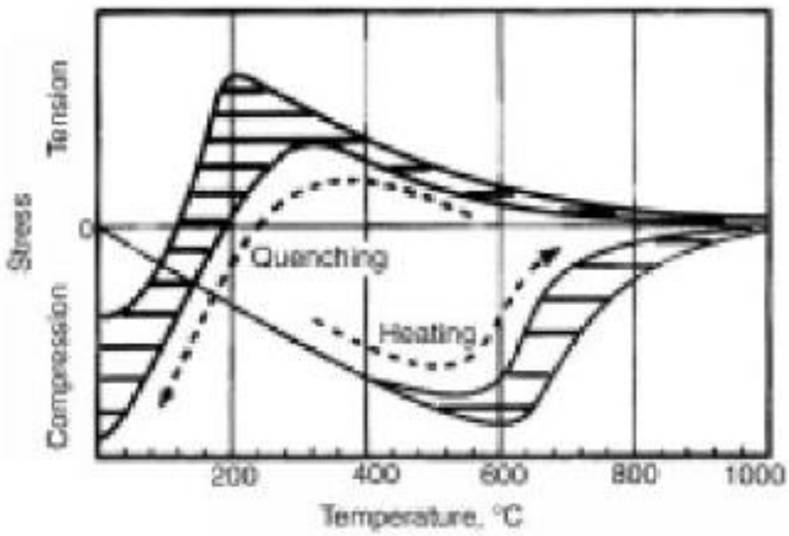


Figure 2.3. Stresses at the surface of a carbon steel cylinder during heating and quenching. Martensitic formation results in a final compressive residual stress state (Weiss, 1999)

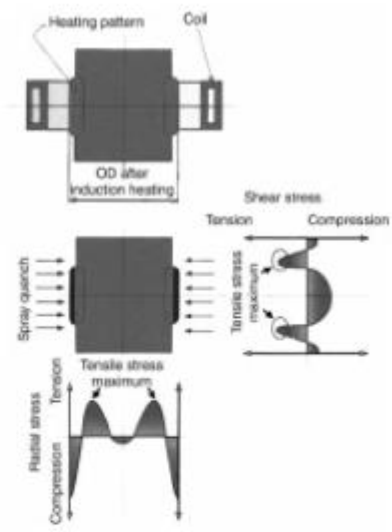


Figure 2.4. Complex pattern of residual stresses forms in a carbon steel cylinder after induction heating and spray quenching. Note: Stresses shown are on a macroscopic scale. OD, outside diameter (Weiss, 1999)

### 3.1.4 Distortion Due to Heat Treating

Distortion can be defined as an irreversible and usually unpredictable dimensional change in the part during heat treating. The term dimensional change is used to denote changes in both size and shape. For purposes of induction heat treatment, distortion is an uncontrolled, irreversible movement that occurs in a part as a result of the heat treating process. The essential intention of the heat treating is to keep the distortion within allowable limits that will enable the part to be completed as designed in the manufacturing process. However, sometimes processes such as tempering, cryogenic processing, straightening, machining, and grinding operations must be used to put the part back into useable tolerances. Figure 2.5 and figure 2.6 show two different types of parts with distortion problems. Both gears have distortion due to size change and shape change. Note that the recommendation for eliminating the distortion in figure 2.5 is to change the design of the gear, whereas for the gear in figure 2.6 the weight holes should be located deeper or should be drilled after the part is hardened.

Size distortion or change in size in the microconstituents due to the volumetric changes that occur during a phase change were previously discussed. Limiting size change can be very important when semi-finished parts are induction hardened and zero net change in size is an objective.

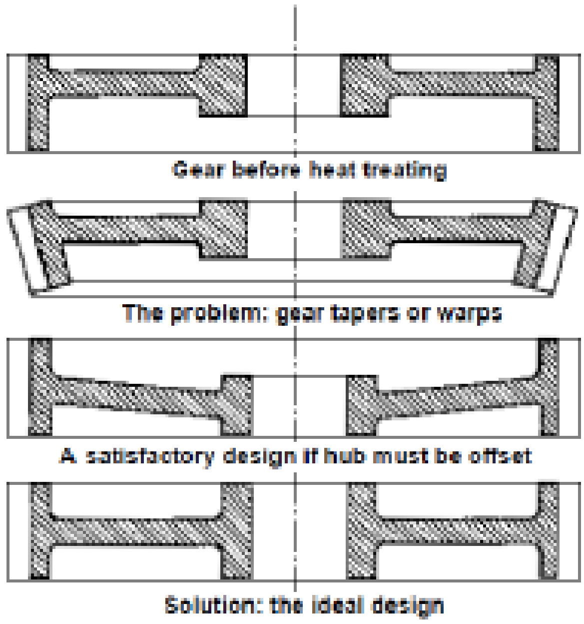


Figure 2.5. Distortion caused by lack of symmetry in a gear. A typical problem caused by lack of symmetry in design, illustrated by a gear that warped during heat-treating (American Society for Metals, 1997)

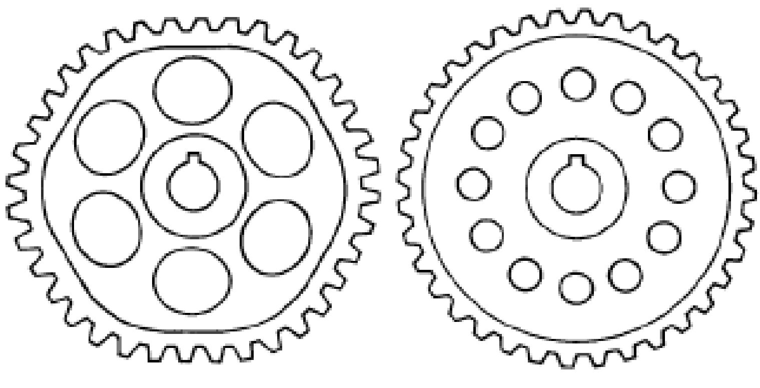

Figure 2.6. Distortion caused by lack of symmetry in a gear. Problem caused by the use of holes to reduce weight of a gear (American Society for Metals, 1997)

Shape change, bending, or warpage are the effects of the residual stresses in parts before they are hardened and the heat treatment hardening process itself can cause distortion due to shape change. Spiral gears may straighten, and shafts may bend. Bores may close, and overall lengths may change (American Society for Metals, 1997).

### 3.1.5 Induction Hardening on Commercial Spur Gear of Mechanical Press Machine

This research investigated the heat treatment process on the commercial spur gear of mechanical press machine. In the real case, the heat treatment process is only conducted in the teeth of spur gear by using induction hardening method shown in the figure 2.7. That is the common method used in the gear heat treatment due to only teeth part need to be hardened. The teeth with high hardenability but minimized residual stress-induced cracking and distortion are the major intent of this process.

Induction hardening is the heat treatment process where the concept of electromagnetic induction is used for heating metallic workpiece, then continued by rapid cooling (quenching) process. This method allows establishing heat treatment only on the specified regions depends on the design of induction coil. Recently, numerous coil design and method have been built, but basically there are two methods of induction hardening, such as spin hardening and contour hardening. Figure 2.8 shows variations of these processes and the resultant hardening patterns. In spin hardening that uses a circular inductor, the teeth are hardened from the tips downward. While such a pattern may be acceptable for splines and some gearing, heavily loaded gears need a hardness pattern that is more like a carburized case. This is achieved with contour hardening.

Figure 2.7. Heat treatment of spur gear’s teeth using induction hardening in the real case

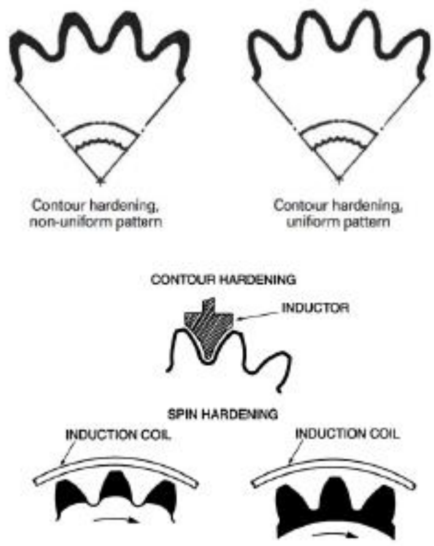


Figure 2.8. Variations in hardening patterns obtainable on gear teeth by induction hardening (Rakhit, 2000)

In order to improve the hardenability of gear teeth, there are two aspects need to be controlled, such as surface hardness and case depth. Frequency and power density of electrical power and its time duration govern the depth of heating, which eventually controls the surface hardness and case depth that can be achieved after induction hardening. Surface hardness is primarily a function of carbon content. It also depends on alloy content, heating time, mass of the gear, and quenching considerations. Hardness achieved is generally between 53 and 55 HRC. The core hardness is developed by quenching and tempering prior to induction hardening, meanwhile the case depth highly depends on the current frequency. Due to flowing current in the induction process is alternating current (AC), the current distribution of entire workpiece is non-uniform with approximately 63% of the current and 86% of the power will be concentrated within a surface, this phenomenon is known as skin effect (Rudnev, et al., 2017). The magnitude of penetration depth of this effect depends on the current frequency inversely. It means that high frequency of current can control heat to a shallow depth on the tooth surfaces, whereas low frequencies produce greater depth of heat penetration. The Figure 2.9 shows the hardening depth of gear teeth generated by different frequencies.

The process sequences of induction hardening is similar to another heat treatment hardening process. However the major difference is the induction hardening occur in the very short time (only few seconds). This condition steers evoluting drastic differences of the case and core microstructures, drastic hardness drop (shown in the figure 2.10), and consequently generating high residual stresses in the case/core interface. Another problems in the induction hardening are difficulty in obtaining uniform case depth on a gear tooth and a reasonable depth of hardness at the center of root fillet. This results in lower bending strength compared with a carburized and hardened gear tooth.

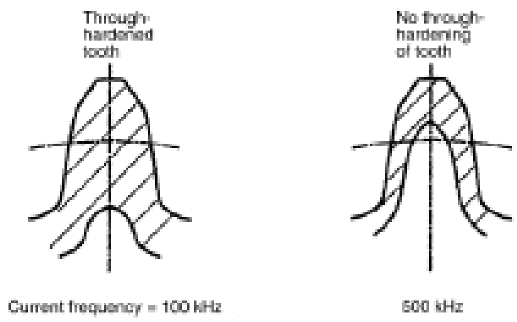


Figure 2.9. Case depth profiles at different current frequency (Rakhit, 2000)

In this real case, the spur gear is heat-treated using single frequency induction hardening with frequency 150 kHz and output power 100 kW. The heating time is around 5 seconds and water spray quenching in 5 seconds with almost no delay time between heating and quenching process. The product results can be seen in the figure 2.11. From the figure, it can be seen that the depth of hardened cases are non-uniform and there are no hardening at the center of root fillet.

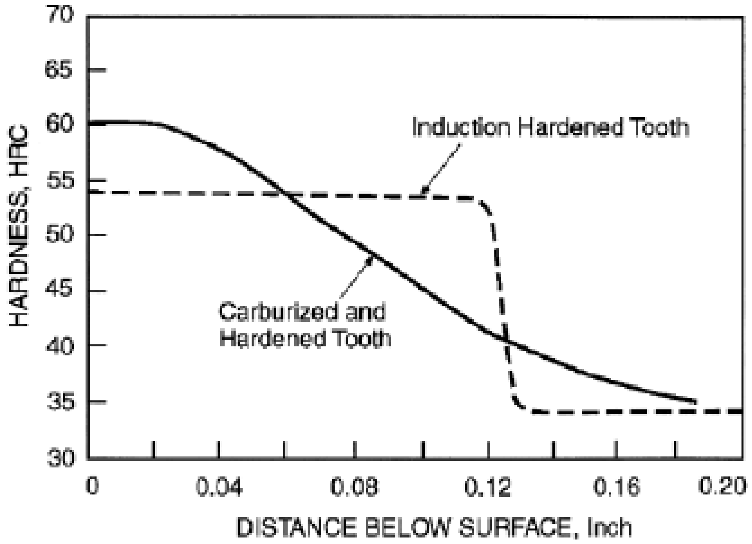


Figure 2.10. Comparison of hardness gradients—induction-hardened and carburized gears (Rakhit, 2000)

(a)

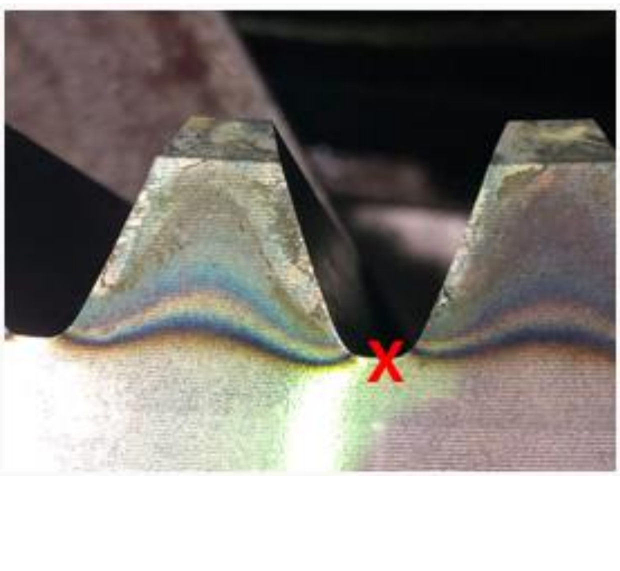

(b)

Figure 2.11. The product results of spur gear induction hardening where (a) non-uniformity in the case depth of the tooth (b) there are no hardening at the center of root fillet

## 2.2 Theoretical Background

The theoretical background of this research comprises of heat treatment mathematical model and computational method. Heat treatment is a multi-physics/multi-scale process during which coupled physical events such as heat transfer, phase transformations and deformation occur simultaneously. The model should considers the process to occur in three distinct physical fields: (1) thermal, (2) metallurgical and (3) mechanical as shown in figure 2.12. The dashed lines in the figure 2.12 mean that the mathematical model of the process is not provided in this research's computational method.

### 2.2.1 Mathematical Model of Temperature Distribution

Appropriate form of Fourier's heat conduction is mathematically established to describe the transient heat transfer within the entire specimen during heat treatment process. Considering that the thermal field is altered by the latent heat of phase transformations, the equation can be expressed in its most general form as,

$$\rho(T)c_p(T)\frac{\partial T}{\partial t} = div(\lambda(T).\nabla T) + Q^{TR}(T,t) \qquad (2.1)$$

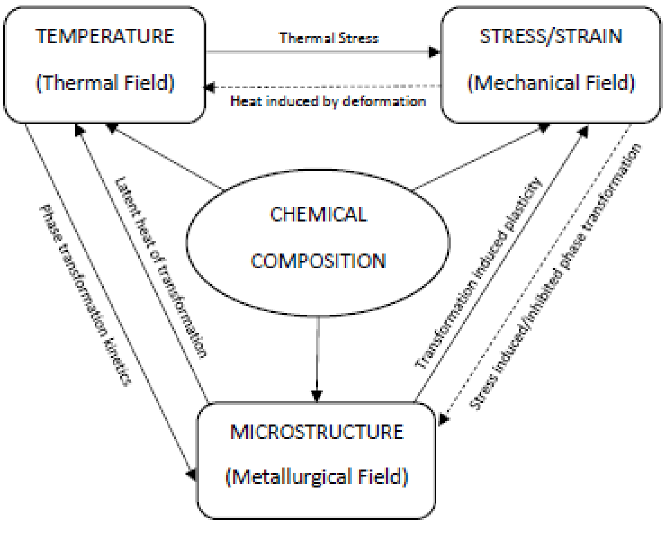

Figure 2.12. Physical fields and the relations in the heat treatment process (Şimşir & Gűr, 2008)

where $\rho(T)$, $c_p(T)$, and $\lambda(T)$ are the density, spesific heat, thermal conductivity of the phase mixture given as a function of temperature respectively, and $Q^{TR}$ is the latent heat released due to phase change. Thermal properties of the phase mixture is approximated by a linear rule of mixture,

$$P(T, \zeta_k) = \sum_1^N p_k \zeta_k \tag{2.2}$$

where P represents a thermal property of the mixture. $p_k$ and $\zeta_k$ are a thermal property and fraction of kth constituent, respectively. To incorporate the effect of latent heat, a fictitious specific heat $(c_p^*)$ is defined as shown on equation 2.3.

$$\left(c_p^*\right) = \sum_{k=1}^N (c_p)_k \, \zeta_k + \sum_{k=1}^N \Delta H_k \frac{d\zeta_k}{dT} = c_p + \sum_{k=1}^N \Delta H_k \frac{d\zeta_k/dt}{dT/dt} \tag{2.3}$$

then, initial and boundary conditions are set to complete the thermal problem definition. The surfaces in contact with the environtment have a film heat transfer boundary condition with surface temperature dependant heat transfer coefficient in the form of

$$\psi(T_s, T_\infty) = h(T_s)(T_s - T_\infty) \tag{2.4}$$

where $T_s, T_\infty, \psi$ and h are surface temperature, environtment temperature, heat flux and temperature depenandt heat transfer coefficient, respectively. Use of a temperature dependent heat transfer coefficient allows simulation of different cooling regimes in different stages of quenching (vapor blanket, nucleate boiling, and convective cooling). Symmetry surfaces and surfaces which are not in contact with environtment are assumed to be insulated surfaces by setting the heat flux to 0 as:

$$\psi = -\lambda \frac{\partial T}{\partial n} = 0 \tag{2.5}$$

### 2.2.2 Mathematical Model of Microstructure Evolution

Microstructural evolution or phase transformation primarily occurs in the quenching process. During quenching process, phase transformation is categorized in two transformation; diffusion-controlled phase transformation (ferrite, pearlite, and bainite evolution) and diffusionless phase transformation (martensitic evolution). These two transformations require different calculation approaches.

2.2.2.1 Diffusion-controlled phase transformation (ferrite, pearlite, and bainite evolution)

Diffusion-controlled transformation is the transformation occur by an incubation period followed by a transformation stage. In order to calculate incubation time required for a diffusional transformation under anisothermal conditions, isothermal transformation diagram (IT) data and Scheil's additivity principle is used. According to Scheil's additivity principle, under anisothermal conditions, incubation is complete when the sum in (2.6) is equal to unity (Scheil, 1935)

$$\sum_{t=0}^{t} \frac{\Delta t_j}{t_s(T_j)} = 1 \tag{2.6}$$

where $\Delta t_j$, $t_s(T_j)$ are the time, step size and time required for the start of transformation under isothermal condition at the current temperature. After the incubation period (S = 1), anisothermal growth kinetics is calculated using a modified Johnson-Mehl-Avrami-Kolmogorov (JMAK) equation (2.7) and Scheil's additivity principle (Johnson & Mehl, 1939)

$$\zeta_k^j = \zeta_k^{max}\left(\zeta_y^{j-1} - \zeta_k^{j-1}\right)\left(1 - exp\left(b_k(T)\tau_j^{n_k(T)}\right)\right) \tag{2.7}$$

where $\zeta_k^j$, $\zeta_y^j$ are volume fraction of kth microstructural constituent and austenite at current (jth) time step. $\zeta_k^0$, $\zeta_k^{max}$ are the initial and maximum fraction of kth microstructural constituent. T is the fictitious time calculated using the transformed amount in the previous time step by

$$\tau_j = \Delta t_j + \left(\frac{-ln\,(1-\zeta_k^{j-1})}{b_k(T)}\right)^{\frac{1}{n_k(T)}} \tag{2.8}$$

$b_k(T)$ and $n_k(T)$ in equation (2.7) are material constants that can be extracted from IT diagram by

$$n_k(T) = \frac{\ln\left[\frac{\ln(1-\zeta_s)}{\ln(1-\zeta_f)}\right]}{\ln\left(\frac{t_s}{t_f}\right)} \tag{2.9}$$

$$b_k(T) = \frac{-\ln\,(1-\zeta_k)}{t_k^{n_k(T)}} \tag{2.10}$$

where $\zeta_s$ and $\zeta_f$ are the fraction of transformed phase at the beginning and at the end of growth stage, which are generally 0.05 and 0.95, respectively.

2.2.2.2 Diffusion-less Phase Transformation (Martensite Evolution)

Martensite is forming by a time independent displacive transformation at temperatures below Ms. Physically, the transformation occurs by nucleation and growth, however; the growth rate is so high that the rate of transformation is almost entirely controlled by the nucleation stage. Volume fraction of transformed martensite is calculated using Koistinen–Marburger equation (2.11) as a function of temperature.

$$\boldsymbol{\zeta_m^j} = \boldsymbol{\zeta_a}(\mathbf{1} - \mathbf{exp}\left(-\boldsymbol{\Omega}\left(\boldsymbol{T_{M_s}} - \boldsymbol{T_j}\right)\right)) \tag{2.11}$$

where $\boldsymbol{\zeta_m}$ is the volume fraction of martensite at current time step and $\boldsymbol{\Omega}$ is a constant. The magnitude of $\boldsymbol{\Omega}$ was found to be $1.10 \times 10^{-2}$; independent from chemical composition for many steels (Koistinen & Marburger, 1959).

2.2.3 Mathematical Model of Stress/Strain Fields

For steel, temperature variation has great effect on elastic and plastic modulus, $\boldsymbol{E_e}$ and $\boldsymbol{E_p}$, while has little effect on Poisson's ratio $\mu$ (Gűr & Tekkaya, 2001) . Therefore, it is assumed that $\mu$ can be considered as a constant while $\boldsymbol{E_e}$ and $\boldsymbol{E_p}$ are functions of temperature in the numerical model.

The generalized Hook law in tensor form is presented as follows:

$$\{\boldsymbol{\sigma}\} = [\mathbf{D_e}]\{\boldsymbol{\varepsilon}_\mathbf{e}\} \tag{2.12}$$

where, $\{\boldsymbol{\sigma}\}, [\boldsymbol{D_e}], \{\boldsymbol{\varepsilon_e}\}$ are stress tensor, elastic matrix, elastic strain tensor, respectively. The total differential equation for (2.12) can be written as:

$$\mathbf{d}\{\boldsymbol{\sigma}\} = [\mathbf{D_e}](\mathbf{d}\{\boldsymbol{\varepsilon}_\mathbf{e}\} - \mathbf{d}\{\boldsymbol{\varepsilon}_\mathbf{0}\}) \tag{2.13}$$

where $\boldsymbol{d}\{\boldsymbol{\varepsilon_0}\}$ indicates additional strain due to the consideration of the effect of temperature on elastic modulus and can be expressed as:

$$\mathbf{d}\{\boldsymbol{\varepsilon}_\mathbf{0}\} = \frac{\boldsymbol{\partial}[\mathbf{D_e}]^{-\mathbf{1}}}{\boldsymbol{\partial}\mathbf{T}}\{\boldsymbol{\sigma}\}\,\mathrm{d}\mathbf{T} \tag{2.14}$$

In the process of quenching, the total strain can be divided into elastic strain $\{\boldsymbol{\varepsilon}_\mathbf{e}\}$, plastic strain $\{\boldsymbol{\varepsilon}_\mathbf{p}\}$, thermal strain $\{\boldsymbol{\varepsilon}_\mathbf{th}\}$, strains due to phase transformation $\{\boldsymbol{\varepsilon}_\mathbf{tr}\}$ and transformation plasticity $\{\boldsymbol{\varepsilon}_\mathbf{tp}\}$. So, the total strain tensor, { }, can be described as:

$$\{\boldsymbol{\varepsilon}\} = \{\boldsymbol{\varepsilon}_\mathbf{e}\} + \{\boldsymbol{\varepsilon}_\mathbf{p}\} + \{\boldsymbol{\varepsilon}_\mathbf{th}\} + \{\boldsymbol{\varepsilon}_\mathbf{tr}\} + \{\boldsymbol{\varepsilon}_\mathbf{tp}\} \tag{2.15}$$

taking into account equation (2.13) produces:

$$\mathbf{d\{\sigma\} = [D_e](d\{\varepsilon\} - d\{\varepsilon_e\} - d\{\varepsilon_p\} - d\{\varepsilon_{th}\} - d\{\varepsilon_{tr}\} - d\{\varepsilon_{tp}\})} \tag{2.16}$$

For a work-hardened material, the yield stress, $\sigma_s$ , is a function of plastic flow and temperature. The initial yield, at which a material will start yielding, can be determined by Von Mises yield criterion which presumes that the plastic flow occurs when the equivalent stress, ( _ ) , equals the yield stress. The criterion for the yield can be expressed as:

$$\boldsymbol{\bar{\sigma} - \sigma_s(\int d\bar{\varepsilon}_p, T) = 0} \tag{2.17}$$

where $\boldsymbol{\bar{\sigma}}$ and $\boldsymbol{\sigma_s}$ are equivalent stress and yield stress, respectively and $\boldsymbol{d\bar{\varepsilon}_p}$ represents the increment of equivalent plastic strain. According to Prandtl–Reuss flow rule (Prandtl, 1924) and (Reuss, 1930), the relationship between incremental plastic strain, $\mathbf{d\{\varepsilon_p\}}$, and stress state can be derived:

$$\mathbf{d\{\varepsilon_p\} = d\{\bar{\varepsilon}_p\}\frac{\partial\bar{\sigma}}{\partial\{\sigma\}}} \tag{2.18}$$

the total differential form of equation 2.17 is:

$$\boldsymbol{\left(\frac{\partial\bar{\sigma}}{\partial\{\sigma\}}\right)^T d\{\sigma\} = \frac{\partial\sigma_s}{\partial\bar{\varepsilon}_p}d\bar{\varepsilon}_p + \frac{\partial\sigma_s}{\partial T}dT} \tag{2.19}$$

Thus, substituting Eqs. (2.16) and (2.18) into Eq. (2.19) gives:

$$\mathbf{d\{\bar{\varepsilon}_p\} = \frac{\left(\frac{\partial\bar{\sigma}}{\partial\{\sigma\}}\right)^T [D_e](d\{\varepsilon\} - d\{\varepsilon_{th}\} - d\{\varepsilon_{tr}\} - d\{\varepsilon_{tp}\} + d\{\varepsilon_0\}) - \frac{\partial\sigma_s}{\partial T}dT}{\frac{\partial\sigma_s}{\partial\bar{\varepsilon}_p} + \left(\frac{\partial\bar{\sigma}}{\partial\{\sigma\}}\right)^T [D_e]\frac{\partial\bar{\sigma}}{\partial\{\sigma\}}}} \tag{2.20}$$

The thermal strain rate can be expressed as:

$$\mathbf{d\{\varepsilon_{th}\} = \textstyle\sum_0^2 f_i\xi_i dT} \tag{2.21}$$

where $\boldsymbol{\xi_i}$ is thermal expansion coefficient of the i th phase. The term $\{\boldsymbol{\varepsilon_{tr}}\}$ corresponds to the mechanical strain resulting from a volume change during the phase transformation:

$$\mathbf{d\{\varepsilon_{tr}\} = \textstyle\sum_0^2 \beta_i(T)df_i} \tag{2.22}$$

$$\boldsymbol{\beta_i(T) = \beta_i(0) + (\xi_i - \xi_{i-1})T} \quad \mathrm{i} \geq 1 \tag{2.23}$$

where $\beta_i(T)$ and $\beta_i(0)$ is structural dilatation due to phase transformation at temperature of T and 0 °C. $\xi_i$ and $\xi_{i-1}$ denote the coefficients of thermal expansion of new phase and parent phase. The model of transformation induced plasticity strain rate applied during the marten- sitic transformation is based on Desalos proposal (Fletcher, 1989), which can be expressed as:

$$\mathbf{d\{\boldsymbol{\varepsilon}_{tp}\} = 3K\{S\}(1 - f_2)df_2} \quad (2.24)$$

where $f_i$ and $\beta_i$ are fraction of parent phase and structural dilatation due to phase transformation of $i^{th}$ phase while K and $\{S\}$ denotes the Desalos parameter of martensite phase transformation and the deviatoric stress tensor.

*(This page is left intentionally blank)*

# CHAPTER 3
# RESEARCH METHODOLOGY

## 3.1 Computational Methodology

The computational method in this research uses commercial finite element method (FEM)-based software named QFORM, which provide mathematical models derived in the previous section. The flowchart of simulation procedures using the software is ilustrated in the figure 3.1.

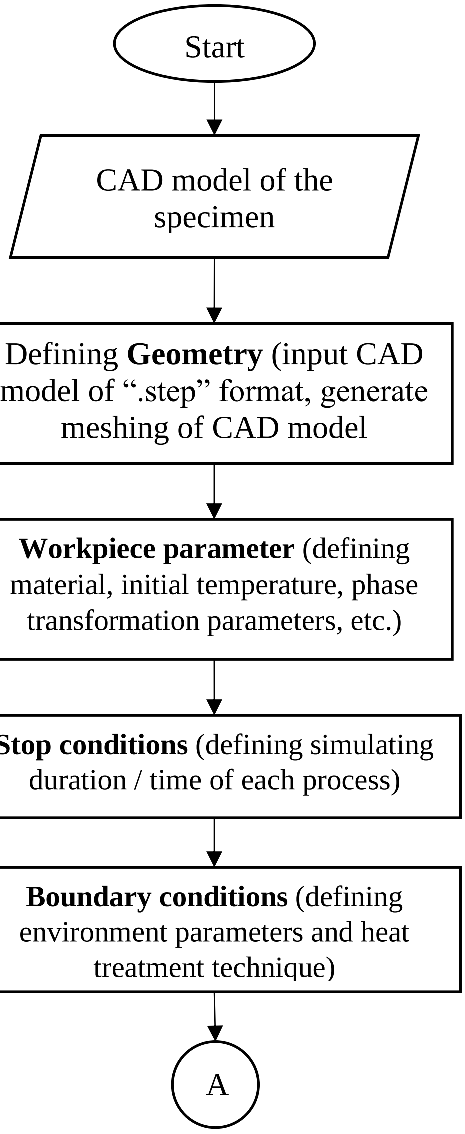

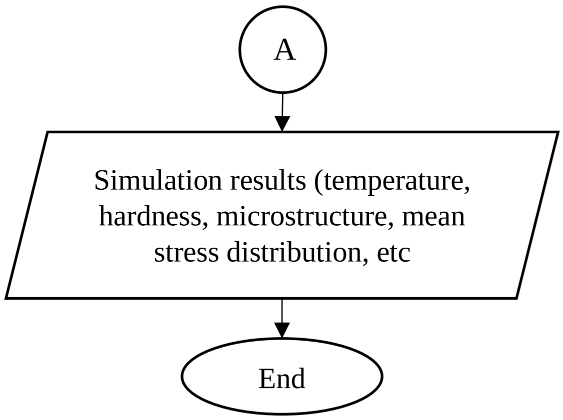


Figure 3.1. Flowchart of computational procedures

### 3.1.6 Defining Geometry

This research simulated a real industrial spur gear design which is engaged with another gears in the commercial mechanical press machine. The scheme of this gearbox is ilustrated in the figure 3.2 where the simulated gear is the largest gear at the bottom. The commercial mechanical press machine is the straight side crank type which adopt design of central driving and 8-point guided slide that increase eccentric loading capacity by 20% with 800 ton punching capacity, 450 mm stroke, and 12-28 SPM (stroke per minute). This kind of machine is applicable for blanking, punching, bending, and forming process of large multi-process which subject the gear teeth to large and impact load. Therefore, hardenability of the gear teeth needs to be improved by induction hardening-heat treatment process to prevent preliminary wear during operating. The geometry, parameters, and finite element of the spur gear are shown in the figure 3.3.

### 3.1.7 Defining Workpiece Parameters

The material used in this research is normalized casting steel SCM440 (JIS standard) with both chemical composition and mechanical properties provided in the software database shown by table 3.1 and figure 3.4 respectively. This initial material which is mostly ferrite and pearlite phase is then transfromed to austenite phase during heating process. The austenite TTT diagram is shown in the figure 3.5 and the data is obtained from calculation based on the chemical composition using Jmatpro software.

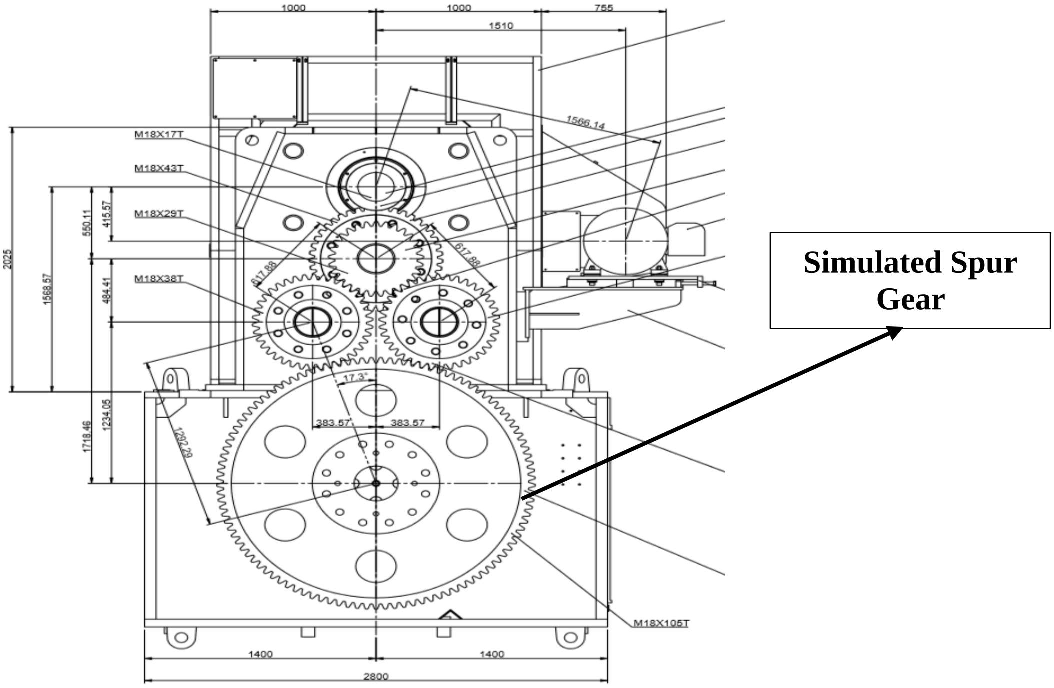


Figure 3.2. The location of simulated spur gear in the gearbox system

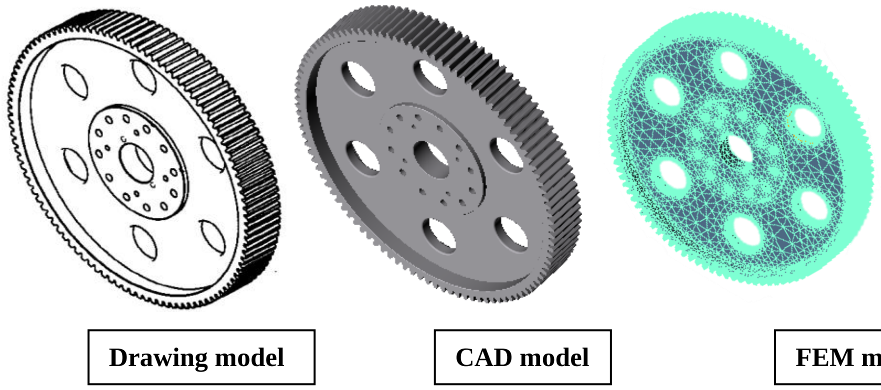


**Gear Parameters**

| | |
|---|---|
| Number of teeth | : 105 |
| Tip circle diameter | : 1925.14 mm |
| Reference circle diameter | : 1889.15 mm |
| Root circle diameter | : 1845 mm |
| Thickness | : 255 mm |
| Module | : 18 |

Figure 3.3. Geometry, parameters, and finite element model of the spur gear

Table 3.1 Chemical composition of the SCM440 material [software database]

| Material | Element (wt%) | | | | | | | |
|---|---|---|---|---|---|---|---|---|
| | C | Si | S | P | Mn | Cr | Mo | Fe |

| | | | | | | | | |
|---|---|---|---|---|---|---|---|---|
| SCM440 | 0.38-0.45 | max 0.4 | max 0.035 | Max 0.035 | 0.6-0.9 | 0.9-1.2 | 0.15-0.3 | Bem |

In the quenching simulation, the austenite phase region is transformed to other phase such as ferrite, pearlite, bainite, and martensite. Based on the chemical composition, software calculate the estimation of phase transformation start temperature during quenching process implementing the calculations from Trzaska’s works (Trzaska, 2016). The hardness distributions is determined by mixture rule from percentage of transformed phase which the hardness value of each phase is obtained from Tartaglia (Tartaglia, et al., 1986) shown in table 3.2 below.

Table 3.2 Estimation of transformation start temperature and hardness of each phases from austenite phase transformation proses

| Phase | Start Temperature ($^0$C) | Hardness (HV) |
|---|---|---|
| Austenite | 860 | 100 |
| Ferrite | 797.194 | 300 |
| Pearlite | 737.865 | 300 |
| Bainite | 540.177 | 500 |
| Martensite | 324.86 | 607.099 |

The percentage of transformed phase during quenching is significantly determined by the cooling rate. The software is implementing the Temperature-time transformation (TTT) diagram for diffusion-controlled phase transformation established by Lee (Lee & Bhadeshia, 1993) shown in figure 3.6 and for difffusionless phase transformation implement the calculation from Koistinen and Marburer (Koistinen & Marburger, 1959) shown in figure 3.7. From those diagrams curves, then software generate the Continous Cooling Transformation (CCT) diagram shown in figure 3.8. The flow stress during austenite and martensite transformation is shown in the figure 3.9.

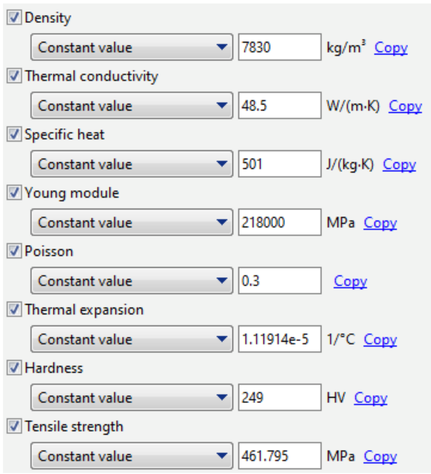


Figure 3.4. Some mechanical properties of normalized SCM440 (software database)

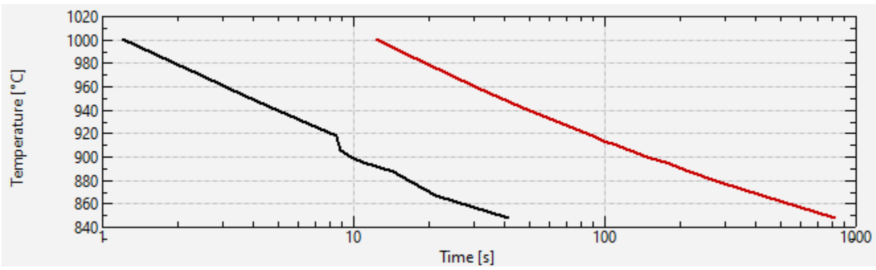


Figure 3.5. Austenite TTT diagram where black line and red line show the start and finish transformation respectively [software interface]

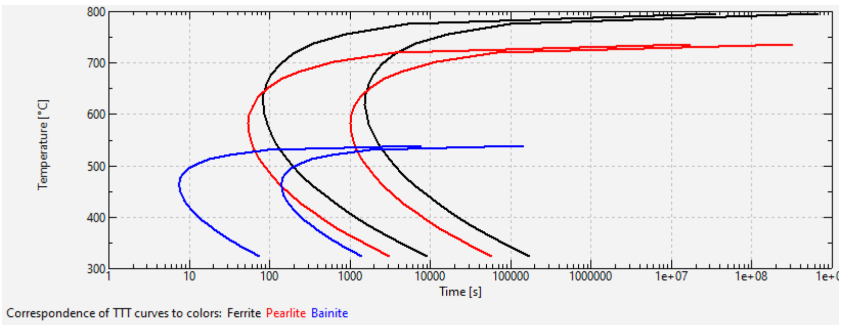


Figure 3.6. TTT diagrams of diffusion-controlled phase transformation [software interface]

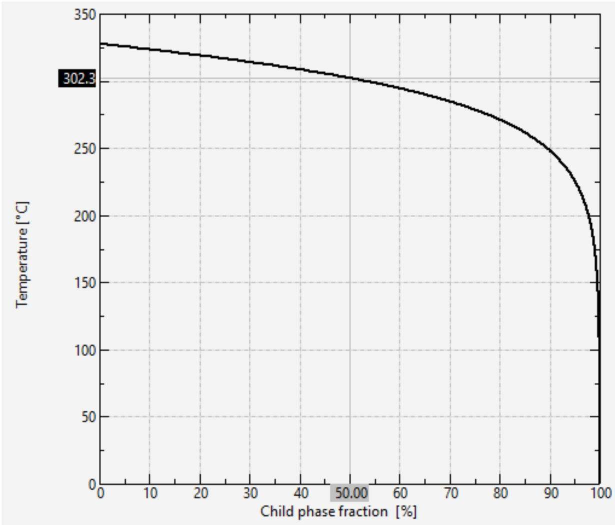


Figure 3.7. Martensitic diagrams of diffusion-less phase transformation [software interface]

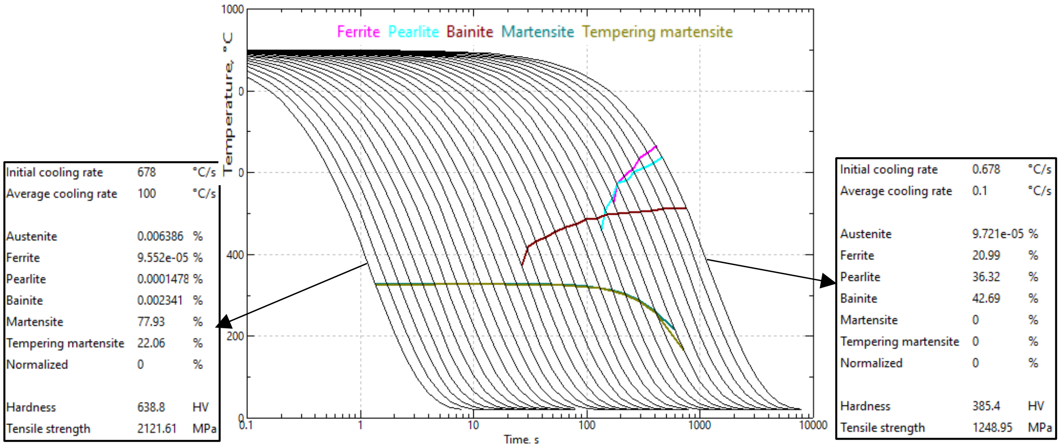


Figure 3.8. CCT diagram [software interface]

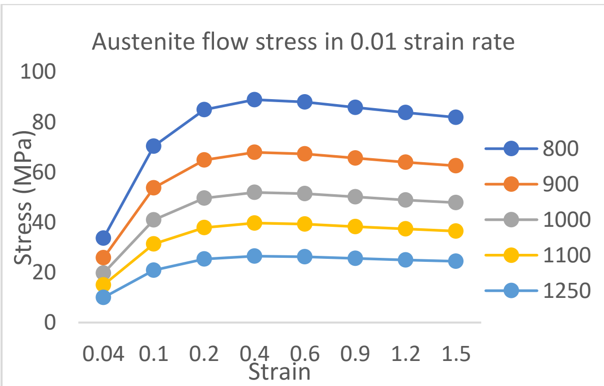

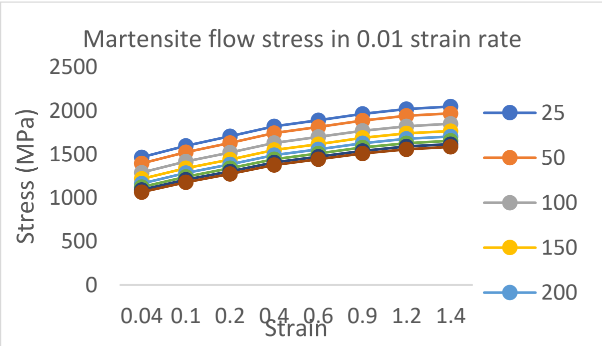


Figure 3.9. Austenite and martensite flow stress of 0.01strain rate for different temperature

### 3.1.8 Stop and Boundary Conditions

There are two important stages in the induction hardening-heat treatment process, such as austenitizing and quenching. All parameters for each process are ilustrated in the figure 3.10. The austenitizing process uses heater database provided in software called salt bath 900$^0$C and quenching process uses water quenchant in temperature 40$^0$C. The heat transfer coefficient of this quenchant is obtained from experimental works (Петраш, 1959) illustrated in the 3.11.

This heat treatment process is only established in the teeth of gear in order to improve the hardenability of the teeth shown in the figure 3.12. The boundary conditions should be set up where the all heat transfer from heater is only subjected to the red area and restrict the gray area only influenced by air heat transfer with temperature 20$^0$C and heat transfer coefficient 30 W/m$^2$K.

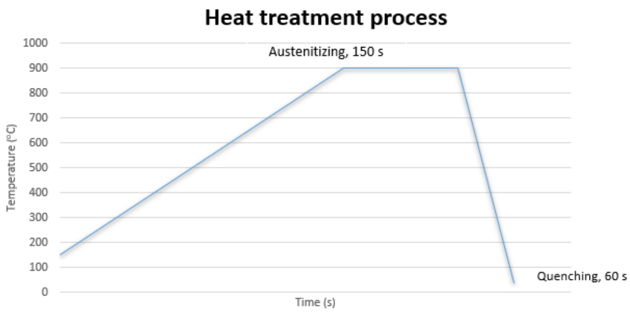


**Medium of Heat Treatment**

**Austenitizing**
Temperature : 900$^0$C
Emissivity : 0.6
Heat Transfer Coeff. : 4000 W/m$^2$.K
**Quenching (Water 40$^0$C)**
Temperature : 40$^0$C
Emissivity : 0.6
Heat Transfer Coeff. : [See figure 24]

Figure 3.10. Temperature-time graph and parameters of the heat treatment medium

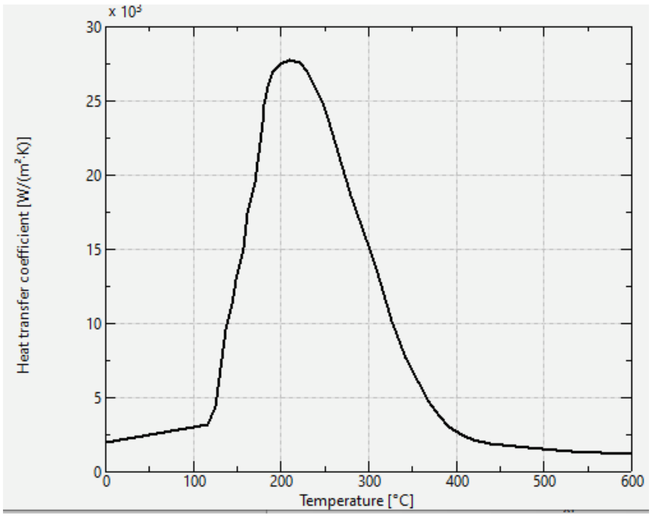


Figure 3.11. Heat transfer coefficient-temperature graph of the water $40^0$ C quenchant [software interface]

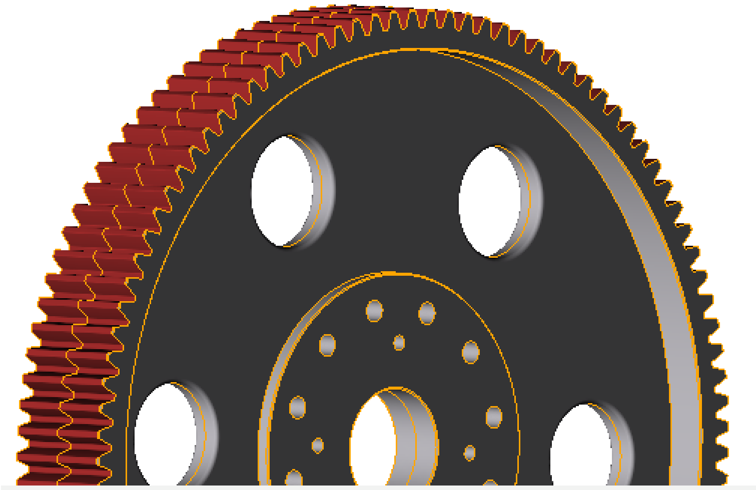

Figure 3.12. Boundary condition of simulation, where the red area is heat-treated area and the gray area is excluded from heater heat transfer

## CHAPTER 4
## RESULT AND DISCUSSION

### 4.1 The Evolution of Temperature

Four points such as tip of tooth's surface (Ts), root of tooth's surface (Rs), tip of tooth's middle cross section (Tm), and root of tooth's middle cross section (Rm) are investigated to analyze the temperature distribution and heating/cooling rate on the teeth of gear. Figure 4.1 shows the temperature-time graph or in other word the heating/cooling rate of those four points in the austenitizing and quenching process and 4.2 describe how the temperature evolutes in the surface and cross middle section during heating and quenching process. As seen from the figures, it can be concluded that the surface regions are heated and cooled relatively similar to the middle cross section regions, where the tip of teeth parts are heated and cooled faster than the root of teeth parts.

These temperature distributions are very reasonable because the heat transfer from environment ignitates from the case transfered to the core of the teeth. Therefore, the case will experience faster heating/cooling rate than the core. Beside that, the tip has the minimum amount of metal heated, compared with the root. Therefore with the same amount of heat rate, the tip will experience more intensive temperature rise/drop than that of root during heating/cooling period as well.

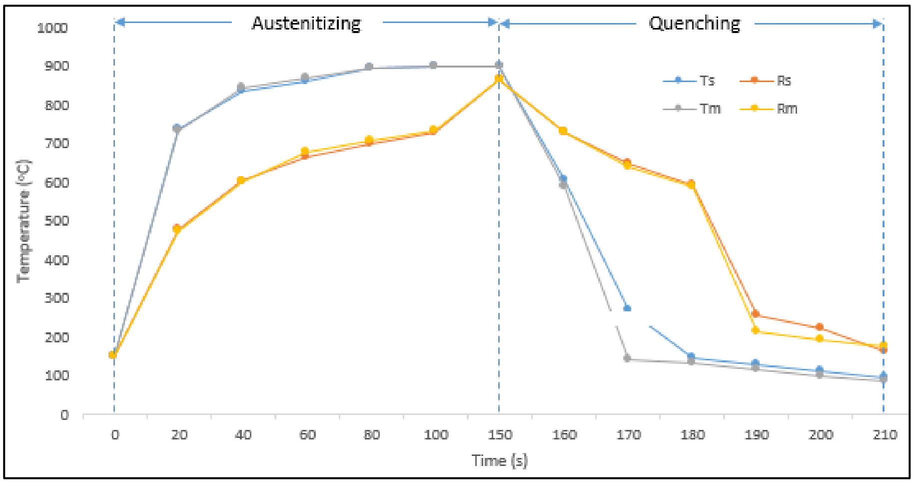

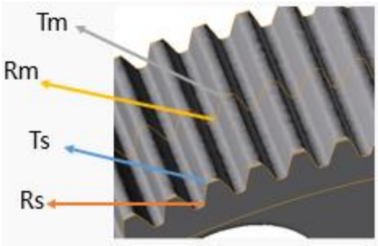


Figure 4.1 Temperature distribution of tooth’s tip and root in both surface and middle cross section for each heat treatment process

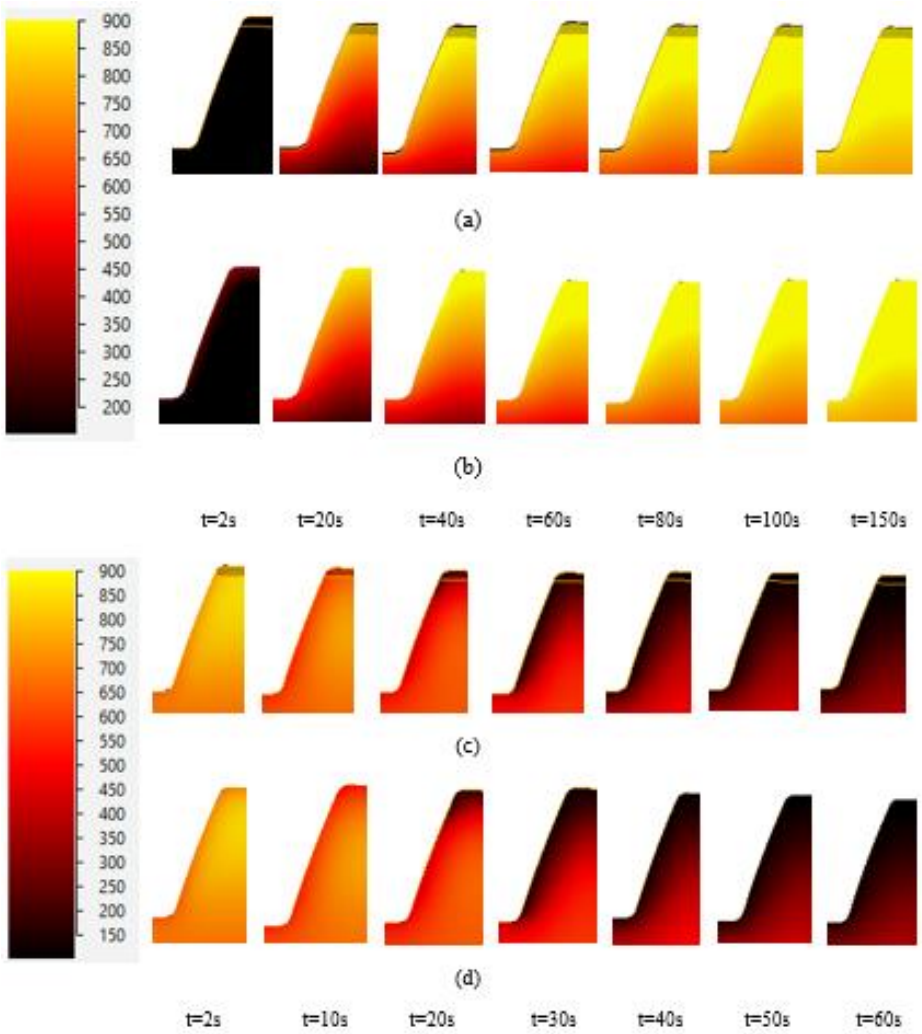


Figure 4.2. Temperature distribution on (a) surface (b) middle cross section of teeth during preheating and (c) surface (d) middle cross section of teeth during quenching

## 4.2 The Phase Transformation

This kind of temperature distribution furthermore generate the phases transformation on the teeth of gear. The final phase distribution in each region is definitely different depends on the heating and cooling rate experienced by each region follow the temperature-time transformation (TTT) diagram explained in the previous chapter.

In the austenitizing process, the initial phase of material (normalized SCM440) which is dominated by ferrite and pearlite phase gradually transform to austenite phase shown in the figure 4.3. The initial phase of material transforms to the austenite phase after the temperature surpass the eutectoid temperature (minimum temperature for austenite) which is about $860^0$ C in this case. In the quenching process, the 100% austenite phase region will be gradually transformed to other phases such as ferrite, pearlite, bainite, and martensite depends on the cooling rate explained by the TTT diagram in the previous chapter. Figure 4.4 shows the evolution of martensite phase on the surface of teeth during quenching process. The martensite evolution starts after 20 seconds quenching time and evolutes gradually from the tip of gear's tooth to the root with the maximum percentage of martensite is about 80%. Comparing this mechanism with the temperature distribution result in the figure 4.2 steers to the conclusion that the heating and cooling rates are the main subjects in the phases transformation. Controlling the phase distribution of material means controlling the heating/cooling rate in each region of material which is not quiet easy task to do.

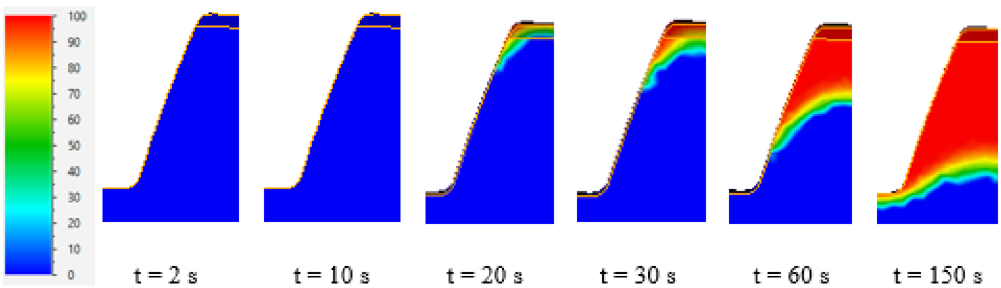


Figure 4.3. Percentage of austenite evolution on the surface of teeth during austenitizing process

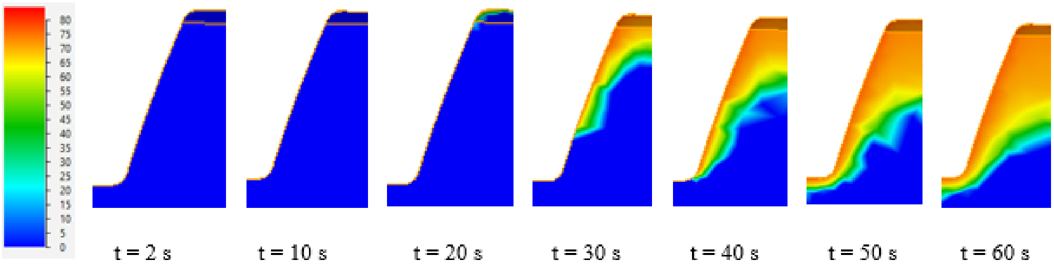


Figure 4.4. Percentage of martensite evolution on the surface of teeth during quenching process

### 4.3 The Evolution of Hardness

As the objective of this research, the hardenability of the teeth needs to be improved by heat treatment process. The hardenability is not only about obtaining desired hardness value, but also controling the hardened depth. Because of it is known that hardening process has big issue with the residual stress which is subjected to the cracking tendency, the hardening distribution should be optimized to improve hardenability but minimize the residual stress distribution.

In the heat treatment process, the hardness value and hardened depth of workpiece highly depend on the quenching process. Because as explained in the chapter 1, the phase transformations occur during rapid cooling process (quenching). The initial austenite phase will be transformed to other phases (ferrite, pearlite, bainite, and martensite) which are harder microstructures than the austenite phase. The hardest phase is martensite phase which is about 2-4 times harder than other phases. Therefore, controling hardened depth means controling the martensite evolution during quenching process. However as mentioned before, controling the martensite distribution during quenching process is not quite simple. Achieving good setting of some parameters, such as carbon content and other elements in the chemical composition of material (carbon equivalent), 100% austenite phase distribution after austenitizing process, cooling rate, quenching medium (quenchant) are needed in order to obtain desired hardenability. This achievement requires numerous trial-error testing and parametric studies as well.

Figure 4.5 ilustrates the simulation result of hardness evolution on the surface of teeth during quenching process. It shows that the presence of martensite (the hardest phase) takes significant role on the overall hardness value where hardness evolution shows similar distribution to the martensite evolution with the maximum hardness is about 645 HV. If it is refered to the temperature distribution in the figure 4.2 then it can be understood that the faster cooling rate regions (black-colored regions) generate greater percentage of martensite transformation then produce greater hardness value. The hardened depth during quenching also need to be investigated so that the residual stress distribution can be measured and controlled to desired value in the future. The figure 4.6 ilustrates the hardened depth during quenching process.

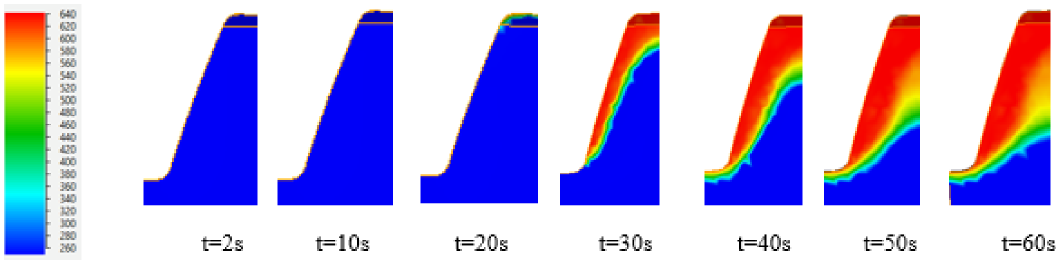


Figure 4.5. Hardness evolution on the surface of teeth during quenching process in HV unit

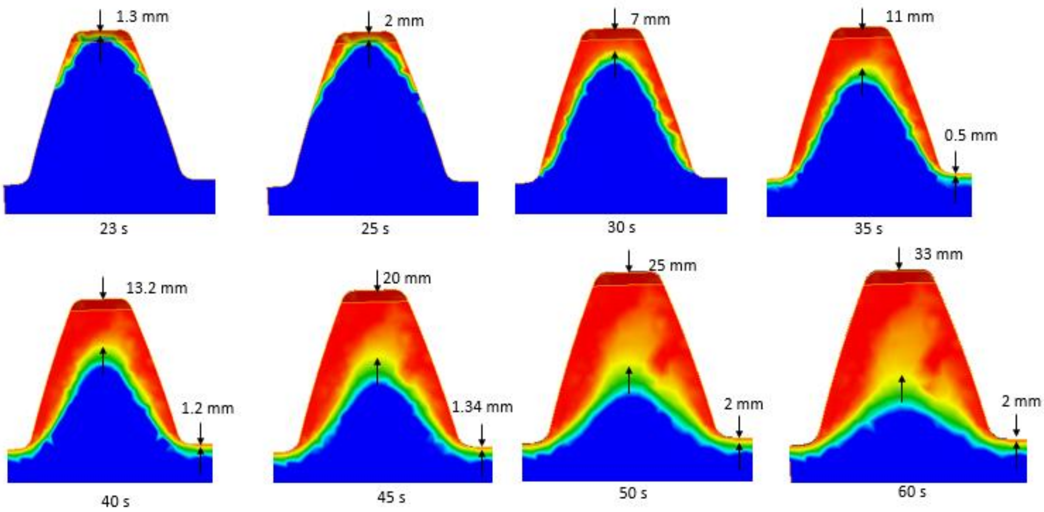


Figure 4.6. The hardened depth of gear's teeth during quenching process

### 4.4 The Hardness Experimental Measurement

These simulation results should be validated or compared to the experimental results to measure the accuracy of this numerical method in predicting the heat treatment process of the gear before establishing numerous heat treatment simulations in order to optimize each parameters of the heat treatment process to obtain the desired results. The validation is conducted by comparing the hardness results on the surface of teeth in both simulation and experimental.

The hardness experimental measurement is established in some points along surface of teeth by using a portable digital hardness tester shown in the figure 4.7. Each point is measured three times and then the mean value is accounted. This comparison result between experimental and 35 seconds quenching simulation can be investigated in the figure 4.8 where  the figure 4.6 plots exact value of the hardness distribution. The hardness value of experimental measurement is in Rockwell C scale (HRC) unit while the simulation one is in the Vickers scale (HV) unit. Therefore, the HV unit in the simulation results should be converted to the HRC unit. However, there is no exact conversion from HV to HRC unit. This research adopts the HV-HRC conversion formula in the low alloy steel established by Hans Qvarnström's work (Qvarnström, 1989) as written in the equation 4.1 and 4.2 below.

$$HV = \frac{223\ x\ HRC + 14500}{100 - HRC} \tag{4.1}$$

Inverse

$$HRC = \frac{100\ x\ HV - 14500}{HV + 223} \tag{4.2}$$

Therefore, based on the graphs in the figure 4.9, It is simply concluded that the simulation result of hardness distribution compared to the measurement results shows similar in trendline but have very significant differences. There are some issues affect this missmatch result. The first is measurement error. It is quite difficult to measure the hardness in exact point position using this tool because the teeth are relatively small compared to probe size of the tool. Beside that, we make some mistakes in measuring such as, we did not measure the 1 mm to 2 mm points below the case which we believe that they have bigger hardness up to 50 HRC (similar to the maximum value of simulated result) and we should measure more than one tooth and calculate the average value regarding in the real case the hardening dept of teeth is not uniform. The second is missmatch parameter data between the simulation and the real case. We believe that parameters data in heater of austenitizing simulation is not apple-to-apple with the induction heater in the real case. The heat transfer coefficient of heater in not large enough to provide fast heating in the case region and generate hardening profile like the real case. Beside that, the maximum hardness value highly depends on the hardness of martensite phase which is different for each paper we read. Further studies need to be conducted to find the adequate hardness value of martensite phase. The third issue is about skin depth phenomenon in the real induction hardening which is quite difficult to be implemented in the simulation procedure.

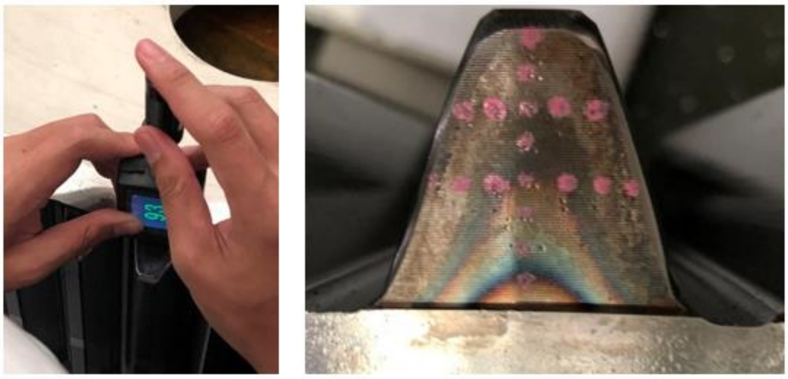

Figure 4.7. The hardness experimental measurement method

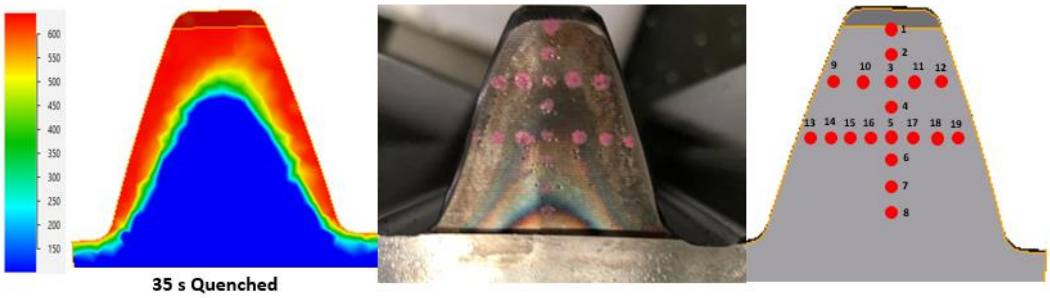


Figure 4.8. Experimental and simulation hardened surface of gear teeth after 40 s quenching process

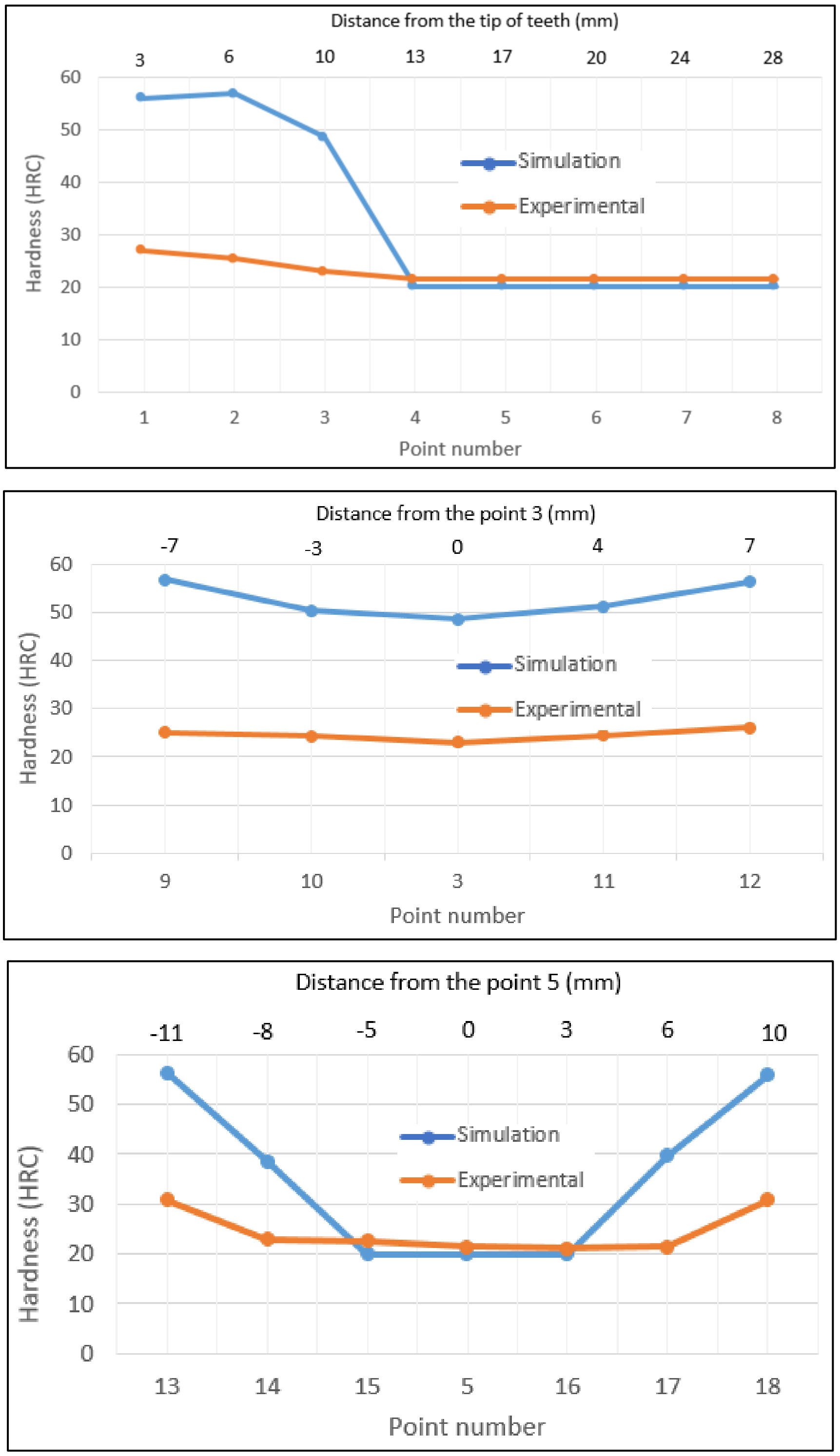


Figure 4.9. Hardness distribution on the surface of gear teeth in the experimental (orange line) and simulation (blue line) result

One of parameter also needs to be considered in quenching process is the quenching medium or known as quenchant. Because of it is known that each quenchant has different heat transfer coefficient which takes significant role in the cooling rate of the workpiece, and the cooling rate significantly influences the martensite evolution and consequently hardness distribution as well. Therefore, this research considers to simulate this heat treatment process using four difference quenchants and analyze the effect of this quenchant subtitution.

In the previous simulation, the water quenchant in temperature $40^0$C is used and the hardness distribution is investigated. The next simulations, same procedure of heat treatment is used with different quenchants., such as new Durixol W72 (oil), new Quenchway 125B (oil), and NaCl 15 pct (brines). The heat transfer coefficient spesification of each quenchant is obtained from the experimental researches (Петраш, 1959) and their comparison is plotted in the figure 4.10. The simulation results are then compared to the water quenching simulation result. The temperature-time graph during quenching process on the tip of teeth surface (Ts point) of those four quenchants is plotted in the figure 4.11. Based on the those two figures, then it is concluded that heat transfer coefficient definitely takes the significant role in the cooling rate of the workpiece. The greater heat transfer coefficient of quenchant used, the faster cooling rate of the workpiece experienced. Not only the temperature distribution, but also martensite and hardness evolution are investigated in the same point. The greater cooling rate generates more percentage of martensite evolution and increase the the hardness value as shown in the figure 4.12. However, by investigating the water and brines quenchant results, it is understood that by changing the greater heat transfer coefficient of quenchant does not significantly increase the maximum value of percentage of martensite evolution and hardness obtained by workpiece. The quenchant with greater heat transfer coefficient only shorten the quenching time in reaching the maximum hardness.

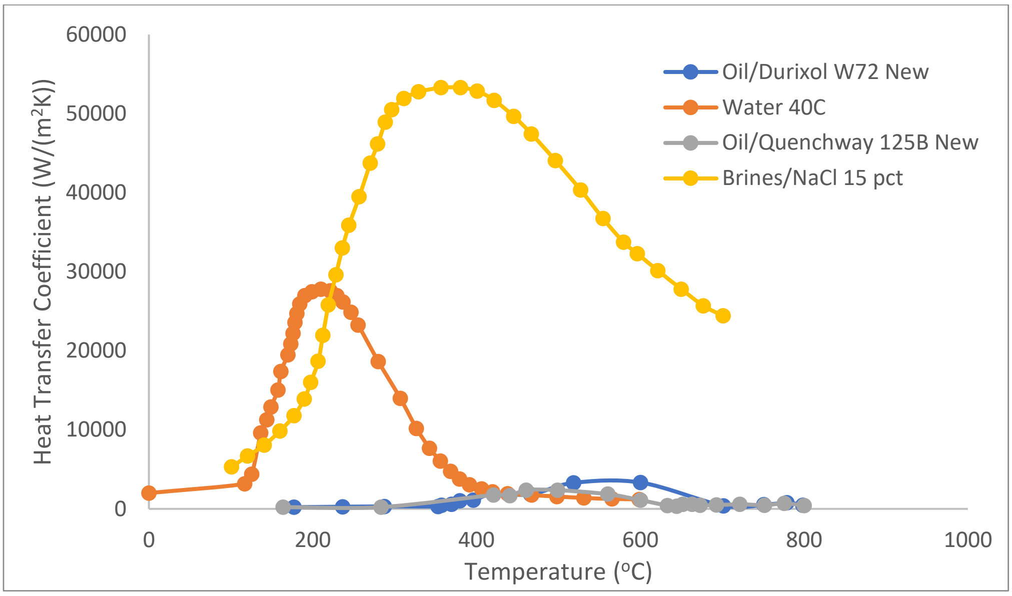


Figure 4.10. Comparison of heat transfer coefficient for each quenchant

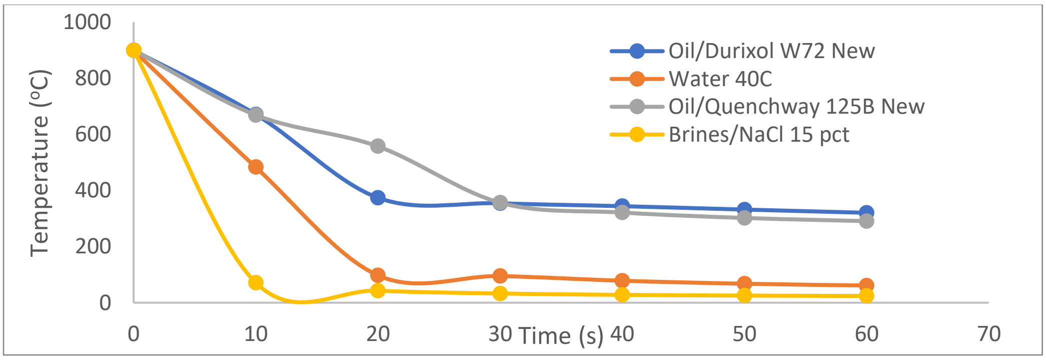


Figure 4.11. Temperature-time graph during quenching process on the Ts point using different quenchants

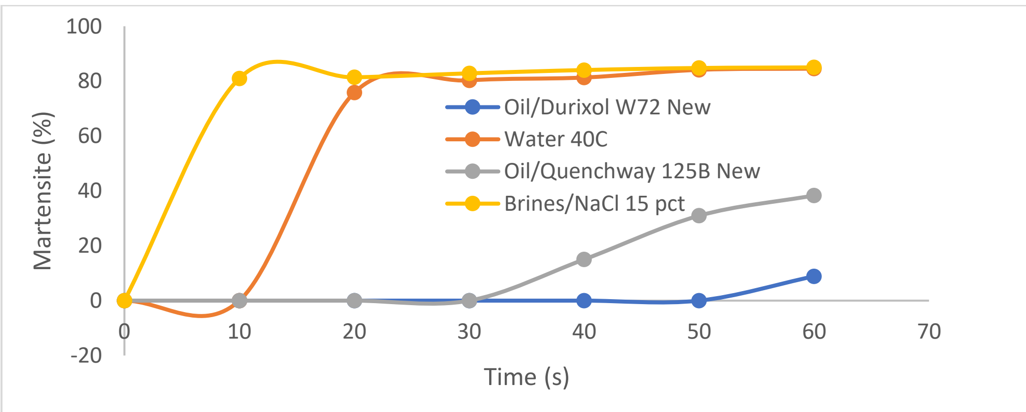

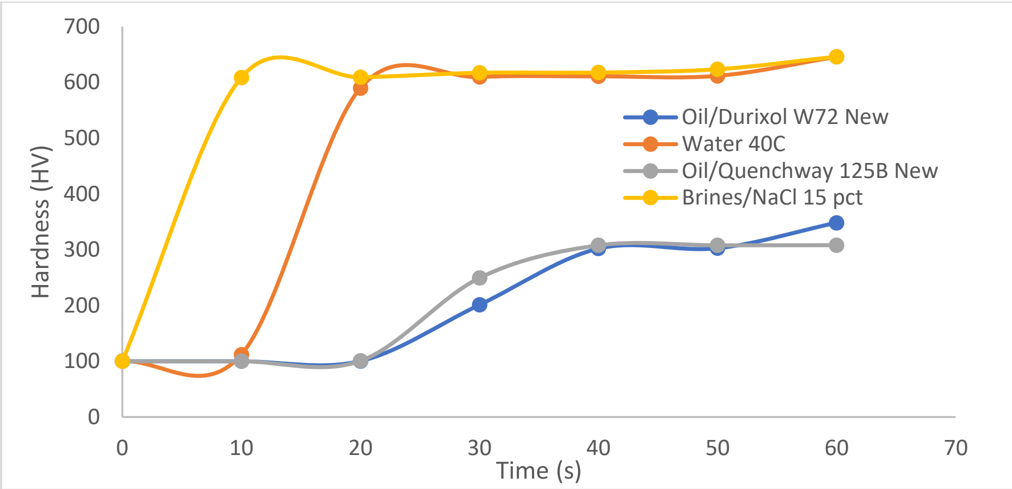


Figure 4.12. Hardness and martensite evolution during quenching process on the Ts point of teeth using different quenchants

### 4.5 The Evolution of Residual Stress

It has been known that mechanism of heat treatment process generate the residual stress in the both case and core of gear which is subjected to cracking tendency. Hardening process may improve gear life in the term of wear resistance, but in other way it can reduce the gear life in term of fatigue life. Therefore it is also essential to design heat treatment process in obtaining appropriate residual compressive stress for beneficial of fatigue life. To understand the stress mechanism during heat treatment process, the middle cross section of teeth (Tm and Rm points) is investigated during heating and quenching process.

During the heating in the austenitizing process, the case is initially subjected to tangensial compression stresses and getting increased due to the thermal expansion of the case and inversely the core will experience the tensile stresses in order to balance mechanism of thermal stress. When austenite starts to form in the case, the magnitude of compression stresses decrease and the tension stresses in core decrease as well. This value keeps decreasing during austenite evolution started from case and even for very long time soaking, the case will inversely experience the tensile stress and the core will experience compression stress, but the value is very small or even close to zero stress (figure 4.13). The austenitizing process commonly leaves the workpiece in the very small residual stress condition in both case and core (neutral stress).

Quenching is suspected as the main role in residual stress induced cracking. At the initial, the outer case cools quickly and experience tangential tension because of thermal contraction while the core will experience tensile stresses to balance the stress (figure 4.14a). These stresses are getting bigger during quenching until at t = 16 s where the tip of teeth (Tm point) experience about 365 Mpa tensile stress and the root of teeth (Rm point) experience about 570 Mpa tensile stress (figure 4.14b). This massive tensile residual stress will generate high cracking tendency in the root of teeth when the root is subjected to external tangensial stresses. At t = 17 s, martensite evolution is getting started from the tip of teeth. This martensite formation generate compressive residual stress in the tip of teeth and generate tensile stresses in the martensite untransformed regions (figure 4.14c). At t = 33 s upon martensite formation and associated volumetric expansion of material in the root, tension in the root is reduced, and compression is getting experienced but in other side, the tip of teeth back to experience tensile stresses in order to balance the core regions which are getting more compressive because of more transformed martensites occur (figure 4.14d). At t = 50s, martensite formation in the root is almost completed, and the stresses are becoming more compressive (figure 4.14e) with about -800 MPa compressive stress and about 265 MPa tensile stress in the tip after 60s quenching. In summary, the mechanism of residual stress in the both tip and root of teeth (Tm and Rm points) is ilustrated in the figure 4.15 where the dashed line in the graph is quenching process and solid line is heating process.

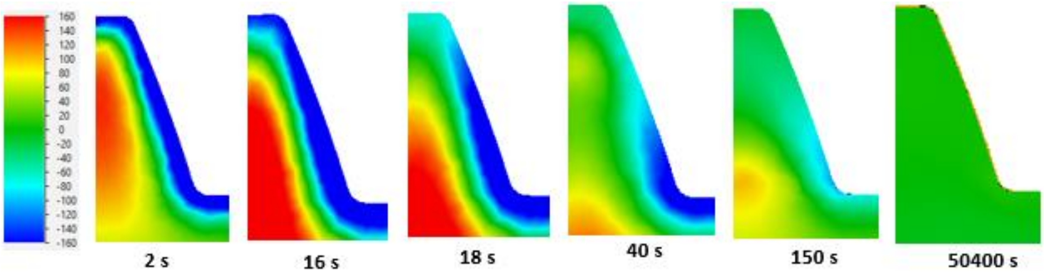


Figure 4.13. Residual stress distribution during austenitizing process

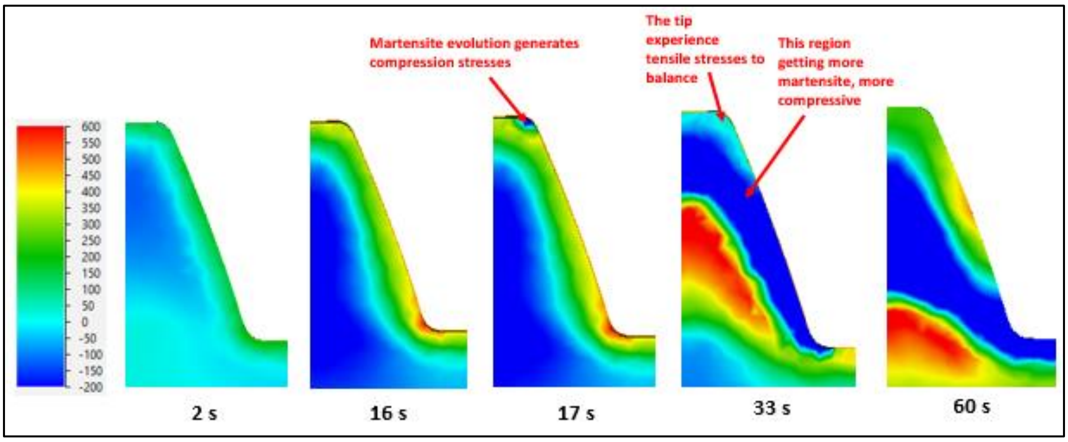


(a) (b) (c) (d) (e)

Figure 4.14. Residual stresses evolution during quenching process in the middle cross section of gear teeth

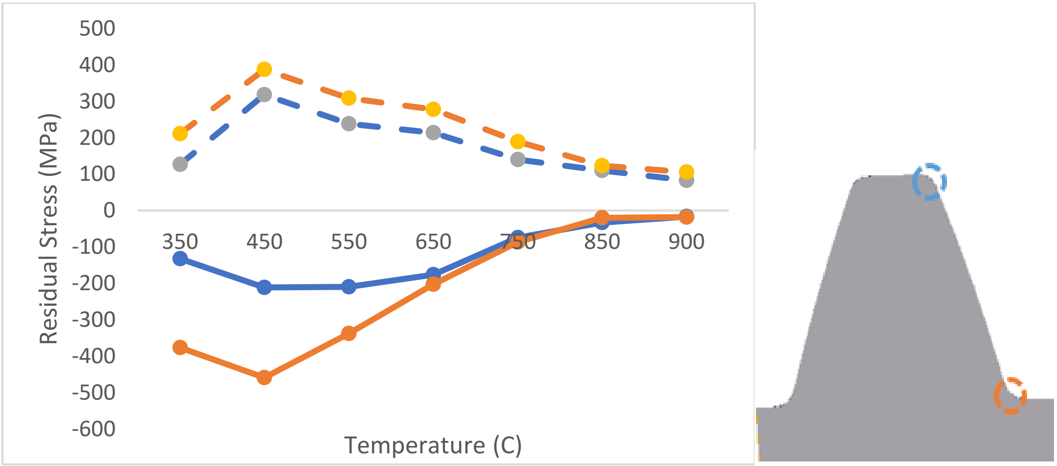


Figure 4.15. Residual stresses of the tip of teeth (blue line) and the root of teeth (orange line) in both heating (solid line) and quenching (dashed line) process

## 4.6 The Investigation of Distribution Possibility in Gear Geometry

In order to understand the behaviour of distortion in the gear geometry after quenching process, the heat treatment process is applied to entire geometry of gear, the parametric study in the design of gear is established, and then the numerical results of volume changes and residual stress in the gear are investigated. The parametric study is established by varying the size of gear’s holes shown in the table 4.1. The geometry and finite element of these four designs are presented in the fig. 4.16.

These designs of gear is subjected to same water quenching process for 60 seconds with the $900^0$ C temperature at the beginning. The volume change results of each design after quenching are presented in the figure 4.17 where the volume changes in the geometry of gear is highly influenced by the presence of the martensite evolution during quenching. The phase transformation from austenite to martensite generates the volume changes of geometry up to 4.338%. When a hole is drilled in the gear, the area around hole will experience direct heat transfer with the environment. This condition generates high cooling rate in the area around hole during quenching which establish massive martensite evolution in this area. The bigger size of hole is definitely bigger area will be transformed to martensite phase. As investigated in the figure 4.17, for holes in design 3 and design 4 are the too close to the teeth where this kind of condition has large possibility to distort the entire shape of gear geometry during quenching process as shown in the figure 2.6. The gear design 3 and 4 should be avoided for quenching process or alternatively the gear's hole should be drilled after heat treatment process. The maximum safety hole size in this case is the gear design 2 where the D/R is equal to 1/3.

Table 4.1 Parametric study in the size of gear's holes

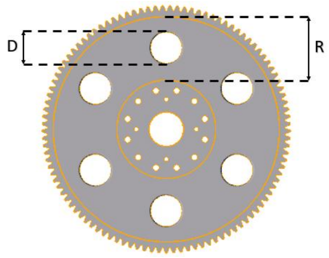


| Gear design | D/R |
|---|---|
| Design 1 | 1/4 |
| Design 2 | 1/3 |
| Design 3 | 1/2 |
| Design 4 | 3/4 |

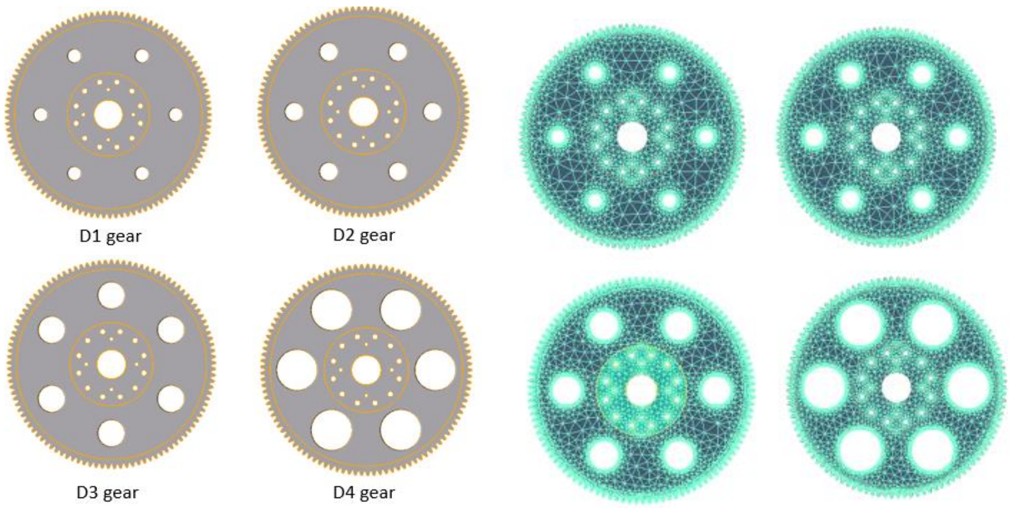


(a) (b)

Figure 4.16. (a) The geometry and (b) finite elements of four gear designs

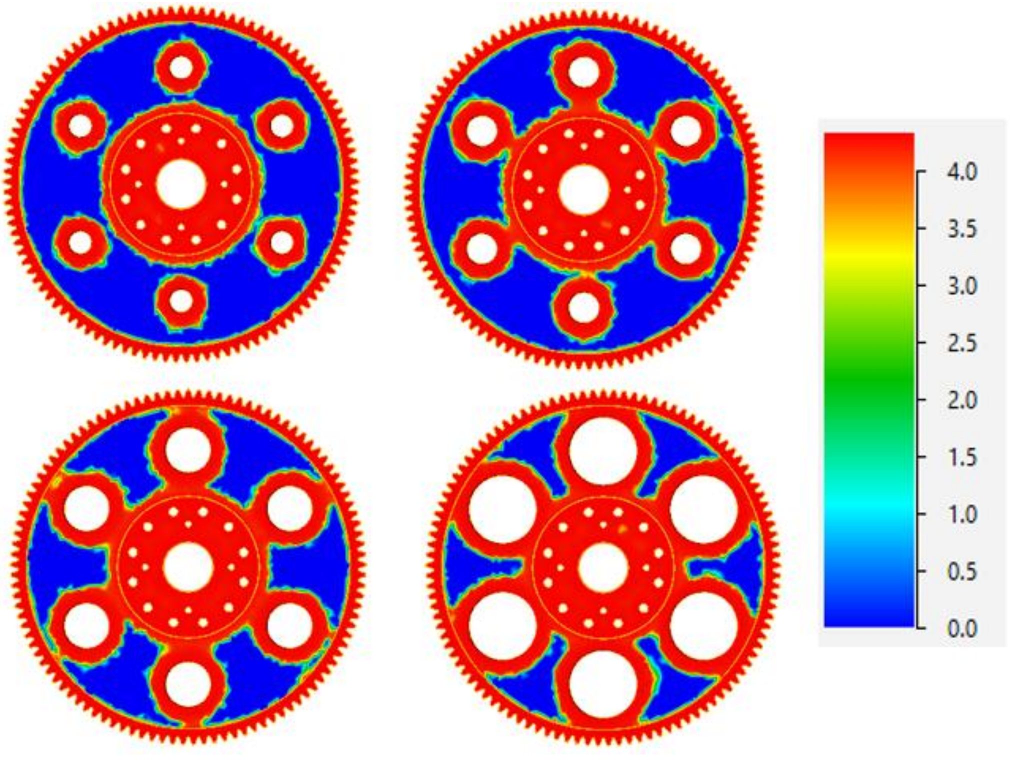


Figure 4.17. The percentage of volume changes in each design after 60 s quenching process

The residual stress results in the core of gear are also investigated to understand the effect of hole geometry to the residual stress. However as shown in the figure 4.18, the residual stress distribution in the four designs are relatively similar. The hole geometry does not give significant effect to the residual stress distribution.

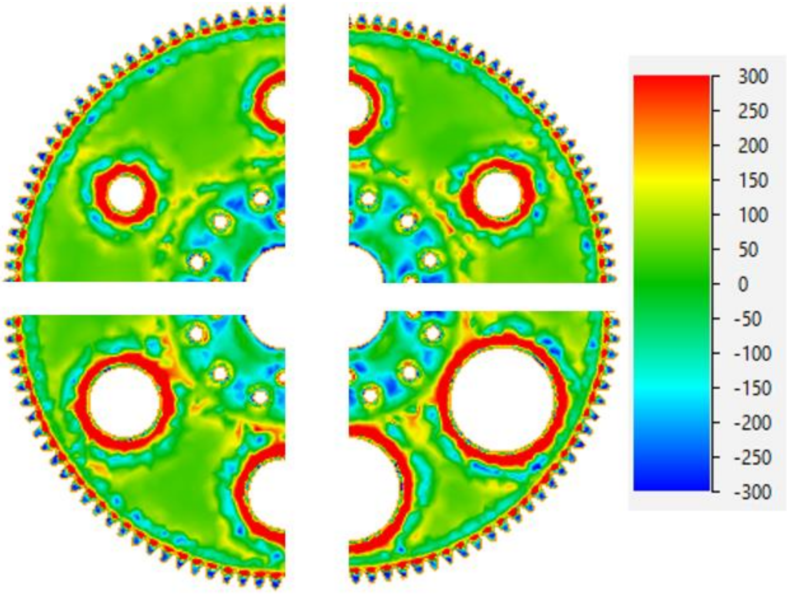


Figure 4.18. Residual stress distribution in the one-fourth geometry of each gear design

# CHAPTER 5
# CONCLUSIONS AND FUTURE WORKS

## 5.1 Conclusion

A numerical method is built to simulate heat treatment process of the spur gear. The evolution of temperature, phase transformation, residual stress, and volume changes (distortion) distribution of gear have been studied according to the simulation results. The experimental validation is also conducted to measure the accuracy of the numerical method in predicting the heat treatment results. Some of conclusions are as follows:

1. The numerical hardness results have similar in trendline but very significant differences compared to the measurement results. This is preliminary attributed by some issues such as measurement error, parameter data mismatch between simulation and the real case, and the skin depth phenomenon in induction hardening which is difficult to be implemented in numerical method
2. Cooling time during quenching takes a big role on the distribution of martensite evolution.
3. Martensite evolution is the main role in the maximum hardness value and hardened depth of the teeth.
4. Change the water quenchant with the higher heat transfer coefficient one does not increase the maximum value of hardness, but shorten the quenching time to reach the maximum value of hardness.
5. After 60 seconds quenching process, the fillet center of root leave residual stress about -800 MPa compressive stress and about 265 MPa tensile stress in the fillet center of tip.
6. The size of hole in the gear gives significant effect to volume changes during quenching process and distortion possibility as well.
7. The size of hole does not give significant effect to the residual distribution in gear geometry.

## 5.2 Future Works

We have poor simulation results in hardness distribution compared to the experimental validation. Further investigations need to be established to improve the accuracy of the numerical method in predicting the real case of induction hardening-heat treatment process.

## References


American Society for Metals, 1973. Metallography, Structures, and Phase Diagrams. In: *Metals Handbook Vol. 8.* s.l.:American Society for Metals.

American Society for Metals, 1991. Heat Treating. In: *ASM Hanbook Vol.4.* s.l.:ASM International.

American Society for Metals, 1997. Material Selection and Design. In: *ASM Handbook Vol. 20.* s.l.:ASM International.

Bain, E. C. & Paxton, H. W., 1961. *Alloying Elements in Steel.* s.l.:American Society for Metals.

Fletcher, A. J., 1989. Thermal stress and strain generation in heat treatment. *Springer.*

Gűr, C. H. & Tekkaya, A. E., 2001. Numerical Investigation of Non-homogenous Plastic Deformation in Quenching Process. *Mater. Sci. Eng. A.,* 164(9), pp. 319-321.

Haimbaugh, R. E., 2001. *Practical Induction Heat Treating.* Ohio, USA: ASM International.

Johnson, W. A. & Mehl, R. F., 1939. *Trans. AIME,* Volume 135, pp. 416-458.

Koistinen, D. P. & Marburger, R. E., 1959. A General Equation Prescribing the Extent of the Austenite-martensite Transformation in Pure Iron-Carbon Alloys and Plain Carbon Steels. *Acta Metall.,* Volume 7, pp. 59-60.

Lee, J. L. & Bhadeshia, H. K. D. H., 1993. A methodology for the prediction of time-temperature-transformation diagrams. *Materials Science and Engineering,* Volume A 171, pp. 223-230.

Prandtl, L., 1924. *Spannungsverteilung in plastischen Körpern.* s.l., s.n.

Qvarnström, H., 1989. Technical Note: A Mathematical Formula for Transformation between Hardness Scales of Rockwell C and Vickers. *J. Heat Treat.,* Volume 7, pp. 65-67.

Rakhit, A. K., 2000. *Heat Treatments of Gear.* s.l.:ASM International.

Reuss, E., 1930. Beruecksichtigung der elastischen Formaenderungen in der plastizitaets- theorie. *Zeitschrift fur Angewandte Mathematik und Mechanik,* Volume 10, pp. 266-274.

Rudnev, V., Loveless, D. & Cook, R. L., 2017. *Handbook of Induction Heating 2nd Edition.* s.l.:CRC Press.

Scheil, E., 1935. *Arch. Eisenhuttenwes,* Volume 12, p. 565.

Şimşir, C. & Gűr, C. H., 2008. 3D FEM simulation of steel quenching and investigation of the effect of asymmetric geometry on residual stress distribution. *Journal of Materials Processing Tech.,* Volume 207, pp. 211-221.

Song, et al., 2007. Numerical Simulation on Carburizing and Quenching of Gear Ring. *Journal of Iron and Steel Research,* 14(6), pp. 47-52.

Song, K. E., Yang, B. C. & Yin, C. S., 2015. Simulation and Analysis of Surface Quenching Process of Spur Gear Based on ANSYS. *IOP Conf. Series: [J] Hot Working Technology*, 44(24), pp. 197-203.
Tartaglia, J. M., Eldis, G. T. & Geissler, J. J., 1986. Hyperbolic Secant Method for Predicting Jominy Hardenability: An Example Using 0.2C-Ni-Cr-Mo Steels. *J. Heat Treating*, 4(4), pp. 352-364.
Trzaska, J., 2016. Empirical Formulae for the Calculation of The Hardness of Steel Cooled from the Austenitizing Temperature. *Arch. Metall. Mater,* 61(3), pp. 981-986.
Wang, et al., 2019. Distortion Control of Large Carburized Gear Shaft Based on Finite Element Analysis. *IOP Conf. Series: [J] Heat Treatment of Metals,* 44(4), pp. 239-242.
Weiss, K., 1999. Induction Tempering of Steel. *Advance Material Processing.*
Zhang, et al., 2016. Finite Element Simulation of Straight Tooth Cylindrical Gear Quenching Based on ANSYS. *IOP Conf. Series: [J] Hot Working Technology,* 45(20), pp. 245-247.
Петраш, Л. В., 1959. Закалочные среды / М.: МАШГИЗ. p. С. 30.